Author Contributions

Conceived and designed the experiments: HH YO. Performed the experiments: HH YO YT MY. Analyzed the data: HH YO YT. Contributed reagents/materials/analysis tools: KT HH. Wrote the paper: HH YO.

References

1. Dykxhoorn DM, Novina CD, Sharp PA (2003) Killing the messenger: short RNAs that silence gene expression. Nat Rev Mol Cell Biol 4: 457–467.
2. Meister G, Tuschl T (2004) Mechanisms of gene silencing by double-stranded RNA. Nature 431: 343–349.
3. Bernstein E, Caudy AA, Hammond SM, Hannon GJ (2001) Role for a bidentate ribonuclease in the initiation step of RNA interference. Nature 409: 363–366.
4. Matranga C, Tomari Y, Shin C, Bartel DP, Zamore PD (2005) Passenger-strand cleavage facilitates assembly of siRNA into Ago2-containing RNAi enzyme complexes. Cell 123: 607–620.
5. Paddison PJ, Silva JM, Conklin DS, Schlabach M, Li M, et al. (2004) A resource for large-scale RNA-interference-based screens in mammals. Nature 428: 427–431.
6. Caplen NJ (2004) Gene therapy progress and prospects. Downregulating gene expression: the impact of RNA interference. Gene Ther 11: 1241–1248.
7. Karagiannis TC, El-Osta A (2005) RNA interference and potential therapeutic applications of short interfering RNAs. Cancer Gene Ther 12: 787–795.
8. Bonini NM, La Spada AR (2005) Silencing polyglutamine degeneration with RNAi. Neuron 48: 715–718.
9. Victor M, Bei Y, Gay F, Calvo D, Mello C, et al. (2002) HAT activity is essential for CBP-1-dependent transcription and differentiation in Caenorhabditis elegans. EMBO Rep 3: 50–55.
10. Wood M, Yin H, McClorey G (2007) Modulating the expression of disease genes with RNA-based therapy. PLoS Genet 3: e109.
11. Miller VM, Xia H, Marrs GL, Gouvion CM, Lee G, et al. (2003) Allele-specific silencing of dominant disease genes. Proc Natl Acad Sci U S A 100: 7195–7200.
12. Miller VM, Gouvion CM, Davidson BL, Paulson HL (2004) Targeting Alzheimer's disease genes with RNA interference: an efficient strategy for silencing mutant alleles. Nucleic Acids Res 32: 661–668.
13. Rodriguez-Lebron E, Paulson HL (2006) Allele-specific RNA interference for neurological disease. Gene Ther 13: 576–581.
14. Maxwell MM, Pasinelli P, Kazantsev AG, Brown RH Jr (2004) RNA interference-mediated silencing of mutant superoxide dismutase rescues cyclosporin A-induced death in cultured neuroblastoma cells. Proc Natl Acad Sci U S A 101: 3178–3183.
15. Denovan-Wright EM, Davidson BL (2006) RNAi: a potential therapy for the dominantly inherited nucleotide repeat diseases. Gene Ther 13: 525–531.
16. Xia H, Mao Q, Eliason SL, Harper SQ, Martins IH, et al. (2004) RNAi suppresses polyglutamine-induced neurodegeneration in a model of spinocerebellar ataxia. Nat Med 10: 816–820.
17. Ohnishi Y, Tokunaga K, Kaneko K, Hohjoh H (2006) Assessment of allele-specific gene silencing by RNA interference with mutant and wild-type reporter alleles. Journal of RNAi and Gene Silencing 2: 154–160.
18. Mullan M, Crawford F, Axelman K, Houlden H, Lilius L, et al. (1992) A pathogenic mutation for probable Alzheimer's disease in the APP gene at the N-terminus of beta-amyloid. Nat Genet 1: 345–347.
19. Goate A, Chartier-Harlin MC, Mullan M, Brown J, Crawford F, et al. (1991) Segregation of a missense mutation in the amyloid precursor protein gene with familial Alzheimer's disease. Nature 349: 704–706.
20. Collinge J (1997) Human prion diseases and bovine spongiform encephalopathy (BSE). Hum Mol Genet 6: 1699–1705.
21. Jackson GS, Collinge J (2001) The molecular pathology of CJD: old and new variants. Mol Pathol 54: 393–399.
22. Prusiner SB (1998) Prions. Proc Natl Acad Sci U S A 95: 13363–13383.
23. Hsiao K, Baker HF, Crow TJ, Poulter M, Owen F, et al. (1989) Linkage of a prion protein missense variant to Gerstmann-Straussler syndrome. Nature 338: 342–345.
24. Yamada M, Itoh Y, Inaba A, Wada Y, Takashima M, et al. (1999) An inherited prion disease with a PrP P105L mutation: clinicopathologic and PrP heterogeneity. Neurology 53: 181–188.
25. Chen SG, Parchi P, Brown P, Capellari S, Zou W, et al. (1997) Allelic origin of the abnormal prion protein isoform in familial prion diseases. Nat Med 3: 1009–1015.
26. Du Q, Thonberg H, Wang J, Wahlestedt C, Liang Z (2005) A systematic analysis of the silencing effects of an active siRNA at all single-nucleotide mismatched target sites. Nucleic Acids Res 33: 1671–1677.
27. Raoul C, Abbas-Terki T, Bensadoun JC, Guillot S, Haase G, et al. (2005) Lentiviral-mediated silencing of SOD1 through RNA interference retards disease onset and progression in a mouse model of ALS. Nat Med 11: 423–428.
28. Singer O, Marr RA, Rockenstein E, Crews L, Coufal NG, et al. (2005) Targeting BACE1 with siRNAs ameliorates Alzheimer disease neuropathology in a transgenic model. Nat Neurosci 8: 1343–1349.
29. Hohjoh H (2004) Enhancement of RNAi activity by improved siRNA duplexes. FEBS Lett 557: 193–198.
30. Ohnishi Y, Tokunaga K, Hohjoh H (2005) Influence of assembly of siRNA elements into RNA-induced silencing complex by fork-siRNA duplex carrying nucleotide mismatches at the 3'- or 5'-end of the sense-stranded siRNA element. Biochem Biophys Res Commun 329: 516–521.
31. Yekta S, Shih IH, Bartel DP (2004) MicroRNA-directed cleavage of HOXB8 mRNA. Science 304: 594–596.
32. Schwarz DS, Ding H, Kennington L, Moore JT, Schelter J, et al. (2006) Designing siRNA that distinguish between genes that differ by a single nucleotide. PLoS Genet 2: e140.
33. Ui-Tei K, Naito Y, Takahashi F, Haraguchi T, Ohki-Hamazaki H, et al. (2004) Guidelines for the selection of highly effective siRNA sequences for mammalian and chick RNA interference. Nucleic Acids Res 32: 936–948.
34. Schwarz DS, Hutvagner G, Du T, Xu Z, Aronin N, et al. (2003) Asymmetry in the assembly of the RNAi enzyme complex. Cell 115: 199–208.
35. Khvorova A, Reynolds A, Jayasena SD (2003) Functional siRNAs and miRNAs exhibit strand bias. Cell 115: 209–216.

Orphan nuclear receptor NR4A2 expressed in T cells from multiple sclerosis mediates production of inflammatory cytokines

Yoshimitsu Doi*, Shinji Oki*†, Tomoko Ozawa*, Hirohiko Hohjoh‡, Sachiko Miyake*, and Takashi Yamamura*†

Departments of *Immunology and ‡Molecular Genetics, National Institute of Neuroscience, National Center of Neurology and Psychiatry, 4-1-1 Ogawahigashi, Kodaira, Tokyo 187-8502, Japan

Communicated by Tadamitsu Kishimoto, Osaka University, Osaka, Japan, April 11, 2008 (received for review March 11, 2008)

Multiple sclerosis (MS) is an autoimmune disease of the central nervous system (CNS) mediated by Th17 and Th1 cells. DNA microarray analysis previously showed that NR4A2, an orphan nuclear receptor, is strongly up-regulated in the peripheral blood T cells of MS. Here, we report that NR4A2 plays a pivotal role for mediating cytokine production from pathogenic T cells. In experimental autoimmune encephalomyelitis (EAE), an animal model of MS, NR4A2, was selectively up-regulated in the T cells isolated from the CNS. Strikingly, a forced expression of NR4A2 augmented promoter activities of IL-17 and IFN-γ genes, leading to an excessive production of these cytokines. Conversely, treatment with siRNA for NR4A2, resulted in a significant reduction in the production of IL-17 and IFN-γ. Furthermore, treatment with NR4A2 siRNA reduced the ability of encephalitogenic T cells to transfer EAE in recipient mice. Thus, NR4A2 is an essential transcription factor for triggering the inflammatory cascade of MS/EAE and may serve as a therapeutic target.

IL-17 | interferon-γ | EAE | Th17 | siRNA

Multiple sclerosis (MS) is a chronic disease of the central nervous system (CNS), accompanying multiple foci of inflammatory lesions. MS is thought to have an autoimmune pathogenesis, involving autoimmune T cells reactive to myelin antigens (1). Development of the CNS inflammation is triggered by proinflammatory cytokines produced by the autoimmune T cells, which penetrate into the CNS parenchyma after being activated in the periphery (2, 3). Although the precise mechanism for the peripheral T cell activation remains obscure, studies indicated possible roles for cross-reactive peptides, cytokines, or superantigen (4).

Experimental autoimmune encephalomyelitis (EAE) is a prototype autoimmune disease model (5) that can be induced in laboratory animals by active immunization with myelin antigens (mAg) or by passive transfer of mAg-specific T cells. Because Th1 cell clones reactive to mAg are capable of inducing clinical and pathological manifestations of EAE in naive mice, it has long been believed that Th1 cells producing IFN-γ play a central role in the pathogenesis of EAE and MS. This postulate is also supported by the past experience that clinical application of IFN-γ treatment for MS turned out to worsen the disease (6). Furthermore, treatment with a peptide analogue of myelin basic protein (MBP) resulted in disease exacerbation along with an expansion of MBP-reactive Th1 cells (7). These results have been repeatedly mentioned to support the Th1-mediated pathogenesis of MS. However, this dogma has recently been challenged. Namely, despite an obvious reduction of Th1 cells, mice deficient for IFN-γ or IFN-γ receptor (8) or for IL-12 signaling were susceptible to EAE (9, 10). Subsequent studies have clarified that IL-23 rather than IL-12 is essential for EAE induction. Lately, the IL-23-dependent pathogenic T cells were identified as Th17 cells, a novel helper T cells producing IL-17 (11, 12). Currently, it is widely appreciated that Th17 cells are crucial in the development of autoimmune diseases either independently or collaboratively with Th1 cells (13).

DNA microarray analysis revealed an up-regulation of IL-17 in the brain lesions of MS (14). More recently, a pathological study has demonstrated that IL-17 secreting T cells are present in active lesions of MS (15). Gene expression profiling provided a number of potential candidate molecules that might be appropriate as a therapeutic target (14, 16). We recently characterized gene signature of peripheral blood T cells from Japanese MS patients and found that a nuclear orphan receptor NR4A2 is most significantly overexpressed in MS (17). NR4A2 mutations are reported to cause familial Parkinson's disease, reflecting its essential role in the development and survival of substantia nigra neurons (18). In contrast, much less attention has been paid onto its role in T cells. NR4A family members (NR4A1 and -3) were shown to mediate apoptotic processes of mature (19, 20) and immature T cells (21, 22). However, these studies do not give insights into an overexpressed NR4A2 in MS. Here, we report that NR4A2 is a transcription factor regulating the expression of key cytokines in the pathogenesis of MS, including IL-17. Furthermore, we revealed that silencing NR4A2 expression by specific siRNA effectively prevents the production of the cytokines, thereby inhibiting their pathogenic potentials to mediate EAE.

Results

Up-Regulation of NR4A2 in Peripheral Blood T Cells of MS. We analyzed gene expression profiles of peripheral blood T cells from MS and control subjects (17, 23). Comparison of the patients and healthy donors has revealed that 286 of 1,263 genes are differentially expressed between MS and controls. Among genes up-regulated in MS, NR4A2 was most significantly overexpressed in MS in statistical P values and an increase ratio (3.6-fold). To consolidate the overexpression of NR4A2 in MS, we performed quantitative RT-PCR for NR4A2 expression, using the same samples previously analyzed. Expression of NR4A2 in T cells from MS increased ≈5-fold on average compared with healthy donors (Fig. 1; $P < 0.01$).

T Cell Expression of NR4A2 in EAE. NR4A2 is a transcription factor of steroid/thyroid receptor family implicated in various cellular responses such as steroidogenesis, neuronal development, atherogenesis, and cell cycle regulation (24). However, its role in

Author contributions: Y.D., S.O., H.H., S.M., and T.Y. designed research; Y.D., S.O., and T.O. performed research; Y.D., S.O., S.M., and T.Y. analyzed data; and S.O. and T.Y. wrote the paper.

The authors declare no conflict of interest.

Freely available online through the PNAS open access option.

†To whom correspondence may be addressed. E-mail: soki@ncnp.go.jp or yamamura@ncnp.go.jp.

This article contains supporting information online at www.pnas.org/cgi/content/full/0803454105/DCSupplemental.

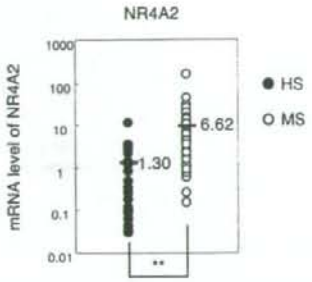

Fig. 1. Quantitative analysis of NR4A2 transcription between MS and controls. CD3⁺ T cells were isolated from PBMC of 57 MS patients and of 19 healthy donors, and total RNA was extracted. cDNA was synthesized and the expression levels of NR4A2 transcript were analyzed by quantitative RT-PCR. Each sample was normalized to GAPDH to adjust for variations. Open circles, MS patients; filled circles, healthy controls. Bars indicate mean values of each group. The statistical difference was determined by two-sided Student *t* test (**, $P < 0.01$).

T cell-mediated autoimmune diseases is unknown. Therefore, we explored the functional involvement of NR4A2 in EAE induced in C57BL/6 (B6) mice by immunization with MOG_{35-55}. CD3⁺ T cells were isolated from SPL, dLN, and PBMC after EAE induction and the expression levels of NR4A2 gene were measured by quantitative RT-PCR (Fig. 2*a Right*). NR4A2 expression was detectable in PBMC-T cells on days 14, 21, and 28, showing a maximum value on day 21, which was well correlated with the clinical severity of EAE (Fig. 2*a Left*). NR4A2 expression in SPL-T cells and dLN-T cells was also correlated with the severity of EAE, but only marginally.

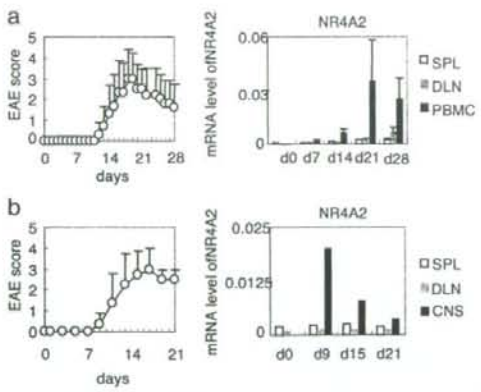

Fig. 2. Kinetic analysis of NR4A2 expression in the disease course of EAE. (*a*) (*Left*) EAE was induced in B6 mice by immunization with MOG_{35-55} in CFA. Mice were killed on days 7, 14, 21 and 28 after immunization, and T cells were isolated from dLN, SPL, or PBMC, using anti-CD3 magnetic beads. (*Right*) Total RNAs were isolated from the T cell populations, and the expression levels of NR4A2 were determined by quantitative RT-PCR. One representative data from three independent experiments is shown, and data are expressed as mean ± SEM ($n = 5$ for each). (*b*) EAE induced in B6 mice with MOG_{35-55}. Clinical scores were expressed as mean ± SEM ($n = 4$). Here, we determined NR4A2 expression in CD3⁺ T cells isolated by using EPICS ALTRA cell sorter. The lymphoid cells (SPL, dLN, and CNS) were pooled from four mice on days 0, 9, 15, and 21 and used for cell sorting and RT-PCR analysis. The purity of the CNS-derived CD3⁺ T cells was >93%.

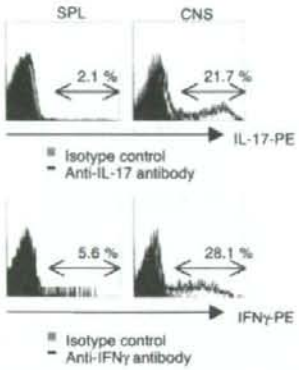

Fig. 3. Accumulation of IL-17 or IFN-γ-producing inflammatory T cells in the CNS. Mononuclear cells were isolated from spleen or CNS on day 17 after immunization and stimulated with PMA (20 ng/ml) and ionomycin (1 μg/ml) in the presence of 2 mM monensin for 4 h. Production of IL-17 and IFN-γ was analyzed for the gated CD4⁺ T cell population by intracellular cytokine staining. Black line represents samples stained with either anti-IL-17 or anti-IFN-γ Ab, and the filled histogram represents samples stained with isotype control. Given values show the percentage of cytokine producing-T cells present in each panel.

In the course of EAE, mAg-primed T cells would accumulate into the CNS and produce inflammatory cytokines, leading to the formation of inflammatory lesions (25). We next examined a kinetic change of NR4A2 in the T cells infiltrating into the CNS. As assessed by quantitative RT-PCR, remarkable expression of NR4A2 was observed in the CNS-T cells on day 9, when an early EAE sign became evident (Fig. 2*b*). The expression level decreased gradually thereafter, but was still significant until day 21. These results suggest that the CNS-T cells also express NR4A2, but the expression kinetics significantly differed from that of PBMC-T cells.

Accumulation of IL-17- and IFN-γ-Producing T Cells in the CNS of EAE. Th1 cells specific for mAg have long been thought to induce EAE through their production of IFN-γ. However, recent studies indicate that Th17 rather than Th1 cells may play a central role (13). To make this point clear in our experimental setting, we examined the ability of the CNS-T cells to produce IFN-γ and IL-17. Mononuclear cells were recovered from the CNS and SPL on day 17, and stimulated with PMA and ionomycin (P/I). After immunostaining, expression of IL-17 or IFN-γ in the CD4⁺ T cells was analyzed by flow cytometry. Major proportions of the CNS-T cells were found to produce IL-17 (21.7% of the cells) or IFN-γ (28.1%) after stimulation (Fig. 3). In contrast, spleen cells contained a lower number of cells producing these cytokines.

Transcriptional Up-Regulation of IL-17 and IFN-γ After Introduction of NR4A2. The concomitant expression of inflammatory cytokines and NR4A2 has guided us to investigate whether NR4A2 directly affects cytokine gene expression as a transcription factor, using luciferase reporter plasmids containing the promoter fragment of IL-17, IFN-γ, or IL-2. NR4A2 gene transduction would result in a twofold augmentation of IL-17 promoter activity and, for IFN-γ, an even higher (5-fold) induction (Fig. 4*a*). A significant induction of IL-2 promoter activity was also noted. Intriguingly, an introduction of NR4A2 plasmid

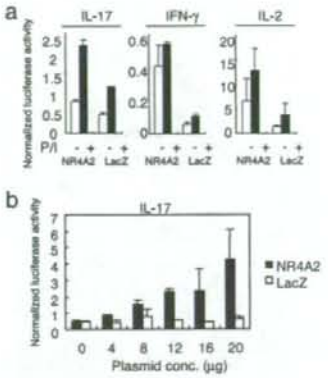

Fig. 4. Promoter activities of cytokine genes in the presence of NR4A2. (*a*) The effect of NR4A2 expression on IL-17, IFN-γ, and IL-2 promoter activity. A reporter plasmid containing promoter of cytokine gene (10 μg) and *Renilla* luciferase plasmid (100 ng) were introduced into EL4 cells by electroporation, together with pcDNA4-NR4A2 or pcDNA4-LacZ (10 μg). Cells were stimulated for 18 h with P/I. Luciferase activity was determined for each cell lysate after normalization to the *Renilla* luciferase activity. One representative data from three independent experiments is shown. Data are expressed as mean ± SD. (*b*) The effect of NR4A2 expression on basal promoter activity of IL-17 gene. EL4 cells transfected with pcDNA4-NR4A2 or pcDNA4-LacZ together with IL-17 reporter plasmid and *Renilla* luciferase plasmid as desribed in *a* were cultured for 18 h without stimulation. One representative data from three independent experiments is shown. Data are expressed as mean ± SD.

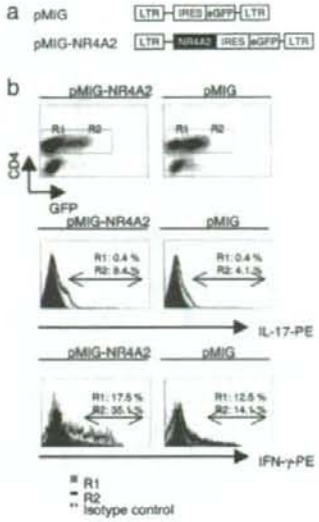

Fig. 5. The effect of retrovirally transduced NR4A2 on cytokine production by primary murine CD4⁺ T cells. (*a*) DNA fragments encoding wild-type NR4A2 were cloned into the pMIG(W) bicistronic retroviral vector. LTR, long terminal repeat; IRES, internal ribosome entry site; eGFP, enhanced green fluorescence protein b. (*b*) Splenic CD4⁺ T cells were infected with retrovirus encoding NR4A2 or control retrovirus, and CD4⁺ GFP⁻ T cells and CD4⁺ GFP⁺ T cells were gated as R1 and R2, respectively. Forced expression of NR4A2 increased the number of CD4⁺ T cells producing IL-17 or IFN-γ. The histogram shows intracellular cytokine staining on the gated cells (R1 or R2). Black line represents cells in R2 gate (GFP+) stained with either anti-IL-17 or anti-IFN-γ Ab, and the filled histogram represents cells in R1 gate (GFP−) stained with isotype control. Given values show the percentage of cytokine producing-T cells present.

without P/I stimulation also augmented basal promoter activity of IL-17 genes in a dose dependent manner (Fig. 4*b*). Similarly, basal promoter activity of IFN-γ was promoted (data not shown).

Retroviral Transduction of NR4A2 Gene Enhances Expression of Inflammatory Cytokine in Primary T Cells. The results obtained in EL4 lymphoma cells need to be verified in more physiological settings. Next, we examined whether forced expression of NR4A2 may affect the expression of cytokines in primary rodent T cells. Bicistronic retroviral vector containing NR4A2 gene fragment (pMIG-NR4A2) or empty vector (pMIG) were used for production of retroviruses (Fig. 5*a*). We infected the B6 T cells with either of the retroviruses as described in ref. 26 and compared the cytokine production between GFP-positive (infected) and GFP-negative (uninfected) CD4⁺ T cells by intracellular cytokine staining (Fig. 5*b Top*). CD4⁺ T cells infected with pMIG-NR4A2-introduced retrovirus showed a twofold enhancement of IL-17 expression (8.4%) compared with those infected with control retrovirus (4.1%) after stimulation with P/I. In contrast, IL-17 production by uninfected T cells in either panel was almost equivalent (Fig. 5*b Middle*). Furthermore, one-third of the CD4⁺ T cells infected with pMIG-NR4A2-introduced retrovirus showed a massive IFN-γ expression (35.1%) compared with control retrovirus (14.1%) (Fig. 5*b Bottom*).

Silencing of NR4A2 Gene Expression Results in a Reduced Production of IL-17 and IFN-γ. Reporter gene analysis and retroviral transduction experiments demonstrated that T cell production of IL-17 and IFN-γ is controlled by NR4A2 (Figs. 4 and 5). We further explored whether silencing of NR4A2 gene may affect the production of inflammatory cytokines by CD4⁺ T cells. An NR4A2-specific siRNA was selected from three siRNAs based on the inhibitory efficacy. The targeting sequence of the NR4A2 siRNA is completely conserved between mice and human. Therefore, we could apply it to human T cells and study whether NR4A2 could be a therapeutic target in human MS. In a preparatory experiment, using FITC-labeled siRNA, the transfection efficiency was found to be 95%. We purified CD4⁺ T cells from human PBMC and transfected them with the NR4A2 siRNA or control RNA, using nucleofector II. The cells were stimulated with immobilized anti-CD3 Ab. As shown in Fig. 6*a*, silencing NR4A2 gene expression resulted in a 50% reduction of IL-17 and IFN-γ production. However, production of TNF-α, IL-4, or IL-5 was not changed significantly after siRNA treatment (Fig. 6*b*). Intriguingly, the siRNA treatment also induced a modest reduction of IL-10 production. The molecular mechanism of this inhibition is not clarified yet. Because silencing of NR4A2 expression rather selectively inhibited the expression of inflammatory cytokines, it is arguable that NR4A2 may be a good target for therapeutic intervention of MS. In this line, we next examined whether the NR4A2 siRNA is effective for inhibiting a production of inflammatory cytokines in MS. For this aim, CD4⁺ T cells were isolated from pairs of an MS patient and an age- and sex-matched healthy donor and were stimulated with anti-CD3 Ab after being transfected with the NR4A2 siRNA or control RNA. We found that the siRNA treatment significantly reduced the production of IL-17 and IFN-γ by T cells from MS or healthy donors [supporting information (SI) Fig. S1]. Again we observed some reduction of IL-10 after siRNA treatment. However, the siRNA showed little effect on

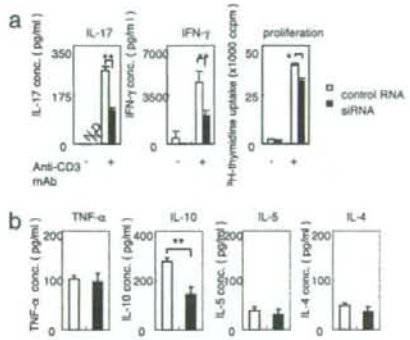

Fig. 6. The effect of NR4A2 gene silencing on T cell cytokine production. (*a*) Specific inhibition of T cell production of IL-17 and IFN-γ by siRNA treatment. Human CD4⁺ T cells derived from PBMC were transfected with siRNA or control RNA and stimulated by immobilized anti-CD3 Ab for 48 h. Cytokine levels in the culture supernatant were determined by ELISA or a CBA human Th1/2 cytokine kit. Proliferation rate was measured by ^{3}H-TdR uptake. (*b*) Effect of siRNA treatment for T cell production of TNF-α, IL-10, IL-5, and IL-4 after stimulation with immobilized anti-CD3 Ab. The data are expressed as mean ± SD (•, $P < 0.05$; ••, $P < 0.01$; Mann–Whitney *U* test).

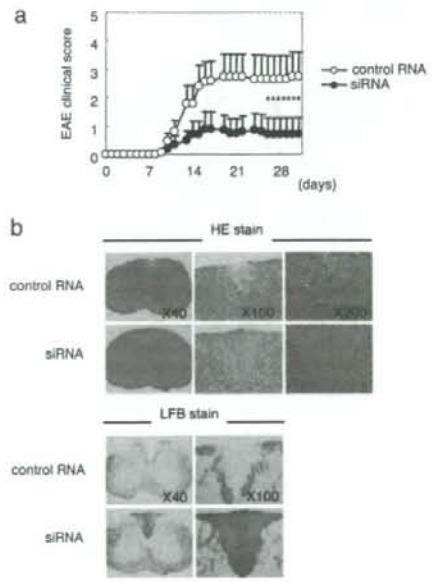

Fig. 7. The effect of T cell silencing of NR4A2 expression on passive EAE. (*a*) Inguinal and popliteal LNs cells were collected from female SJL/J mice 10 days after immunization with $PLP_{139-151}$, and were transfected with siRNA for NR4A2 or control RNA, using HVJ-E vector kit. The cells were cultured in complete media for 8 h. Then the media were replaced with fresh complete media containing 35 μg/ml $PLP_{139-151}$, and the cells were stimulated for another 3 days. After expansion, cells were harvested and transferred i.p. (5×10^6 cells per mouse) into 3Gy-irradiated naïve SJL/J mice ($n = 10$) followed by i.p. injection of PT. Mean ± SEM clinical scores were indicated. (•, $P < 0.05$ by Mann–Whitney *U* test.) (*b*) Histological analysis of spinal cords removed on day 31 after adoptive transfer of $PLP_{139-151}$-reactive T cells. Sections obtained from cervical cord regions were stained with HE or LFB. Infiltration of mononuclear cells and demyelination of the cervical cord regions were analyzed for mice injected with $PLP_{139-151}$-reactive T cells pretreated with control RNA or siRNA for NR4A2.

production of TNF-α, IL-5, and IL-4 from T cells used for assays (Table S1).

Amelioration of EAE by Silencing of NR4A2. Finally, we investigated the therapeutic implication of the siRNA experiments in a model of passively induced EAE, induced by adoptive transfer of mAg-activated LN cells. We prepared lymphoid cells from dLN of SJL/J mice 10 days after immunization with $PLP_{139-151}$. The dLN cells were transfected with the NR4A2 siRNA or control RNA and stimulated with $PLP_{139-151}$ *in vitro*. Three days later, the cultured cells enriched in lymphoblasts were transferred to irradiated naïve SJL/J mice. In addition to evaluating clinical manifestations, histology was assessed by hematoxylin-eosin (HE) and luxol fast blue (LFB) staining of paraffin-embedded spinal cord sections. Notably, severity of clinical (Fig. 7*a*) and histological EAE on day 31 (Fig. 7*b*) was significantly prevented in siRNA-treated group compared with control RNA-treated group (Fig. 7*b*). These results suggest that modulation of NR4A2 expression by specific siRNAs or other chemical compounds might be a promising treatment for active MS that are harboring potent encephalitogenic T cells.

Discussion

Although mAg-specific T cell clones isolated from the peripheral blood has been widely used to gain insights into the pathogenesis of MS (27), analysis of polyclonal T cells has been undervalued for a long time. However, it was recently demonstrated that peripheral T cells from MS and healthy subjects significantly differ in surface phenotype or gene expression profiling (17, 23, 28). Using cDNA microarray, we have identified NR4A2 as a gene most significantly up-regulated in the peripheral T cells of MS (17). We conducted the present study to clarify the implication of this interesting observation. Inspired by the recent discovery that retinoid-related orphan receptor γt (RORγt) is essential for Th17 cell differentiation (29) and that retinoic acids play a regulatory role in Th17 cell differentiation (30), we have focused our efforts to explore the possible role of NR4A2 in cytokine regulation. Reporter gene analysis and retroviral transduction of NR4A2 clearly demonstrated that T cell production of inflammatory cytokines, including IL-17 and IFN-γ, is regulated by NR4A2, whereas silencing of NR4A2 by a specific siRNA prevents expression of these cytokines. Furthermore, treatment with the siRNA reduced the ability of pathogenic T cells to adoptively transfer EAE. These results have identified a previously uncharacterized role for NR4A2 in the regulation of T cell production of inflammatory cytokines.

NR4A2 is a member of the orphan nuclear NR4A subfamily that consists of NR4A1 (also referred to as Nur77), NR4A2 (Nurr1), and NR4A3 (NOR-1) (24). The NR4A members share a highly conserved zing finger DNA binding domain and a less conserved putative ligand-binding domain. All these members bind to the DNA sequence NBRE (AAAGGTCA) or NurRE to activate target gene expression. NR4A1 and NR4A2 can also heterodimerize with retinoic X receptor (RXR) and activate gene expression through DR5 (24). They exert pleiotropic functions and are classified as immediate early genes induced by physiological and physical stimuli. Studies of gene-targeted mice have shown that NR4A1 and NR4A3 play a critical role in T cell apoptosis during the thymocyte development (20–22, 31). In contrast, developing thymocytes in NR4A2 deficient mice ap-

pear to be normal (21, 32), which distinguishes NR4A2 from other NR4A members.

Involvement of orphan nuclear receptor in T cell differentiation has recently attracted broad attention, because RORγt, a splice variant of RORγ, was found to play an essential role in the development of Th17 cells (29). RORγ/RORγt were reported to play an essential function in survival of $CD4^+CD8^+$ thymocytes (33, 34) and in the generation of fetal lymphoid tissue inducer (LTi) cells (35). It is particularly intriguing that the consensus binding sequence for RORγ [$(A/T)_5$AGGTCA] overlaps with that for NR4A (NBRE; AAAGGTCA), which has encouraged us to explore the functional role of NR4A2 in the production of IL-17 and IFN-γ. Although the molecular mechanism of cytokine production through the induced expression of NR4A2 is not clear yet, NR4A2 and RORγt may have an overlapping role in regulating the development and effector functions of Th17 cells.

NR4A2 expression in the CNS-infiltrating T cells showed a peak value at a very early phase of EAE (day 9–12) (Fig. 2*b*). We speculate that this probably coincides with the entry of encephalitogenic cells into the CNS (2, 3). Consistently, a similar kinetic change was found in expression of T-bet and RORγt in the CNS-T cells (data not shown). In contrast, up-regulation of NR4A2 in peripheral blood T cells was significantly delayed. This is likely to result from a late activation of peripheral T cells after peripheral recruitment of antigen presenting cells engulfing myelin and/or peripheral dispersion of myelin protein or its fragments.

By applying a specific siRNA, we showed that blocking NR4A2 expression is effective for inhibiting production of IL-17 and IFN-γ from T cells from healthy donors and MS patients. Therapeutic implication was further demonstrated by using an adoptive transfer EAE model. Because Th17 cells were identified as a major player in autoimmunity (12, 15), it is sometimes argued that Th17 cells would be a sole potent inducer of autoimmune inflammation. However, T-bet-deficient mice and Stat4-deficient mice that obviously lack Th1 cells would resist against induction of EAE, although they maintain a large number of Th17 cells (36, 37). This suggests that both Th1 and Th17 cells are required for induction of full-blown EAE (38). In this context, the ability of the NR4A2 siRNA to inhibit production of both IL-17 and IFN-γ suggests the advantage of NR4A2 targeting therapy in controlling autoimmune inflammation.

Materials and Methods

EAE Induction. Active EAE was induced with myelin oligodendrocyte glycoprotein (MOG) amino acids 35–55 (MOG_{35-55}; MEVGWYRSPFSRVVHLYRNGK) as described in ref. 39. Female B6 mice were immunized s.c. with 100 μg of MOG_{35-55} mixed with 1 mg of heat-killed *Mycobacterium tuberculosis* H37RA emulsified in Freund's adjuvant (CFA). Pertussis toxin (PT) (200 ng) was injected i.p. on days 0 and 2 after immunization. Clinical signs were scored daily as follows: 0, no clinical signs; 1, loss of tail tonicity; 2, flaccid tail; 3, partial hind limb paralysis; 4, total hind limb paralysis; and 5, fore and hind limb paralysis.

Quantitative RT-PCR. DNase-treated total RNAs were processed for cDNA synthesis, using random hexamer primers and SuperScript II reverse transcriptase (Invitrogen). cDNAs were amplified by PCR on Light Cycler ST300 (Roche Diagnostics) by using a Light Cycler-FastStart DNA Master SYBR Green I kit (Roche). Values for each gene were normalized to those of a housekeeping gene GAPDH to adjust for variations between different samples. Forward primer for amplifying human NR4A2 gene was 5′-CGACATTTCTGCCTTCTCC-3′ and reverse primer 5′-GGTAAAGTGTCCAGGAAAAG-3′. Mouse NR4A2 forward primer was designed as 5′-GCATACAGGTCCAACCCAGT-3′ and reverse primer 5′-AATGCAGGAGAAGGCAGAAA-3′. To evaluate silencing efficacy of *NR4A2*-specific siRNAs, expression of NR4A2 gene was quantified by RT-PCR, using the primers to flank the siRNA target sequence (forward, 5′-TGCCACCACTTCTCTCCCCA-3′; reverse, 5′-GCGGCATCATCTCCTCAGAC-3′).

Luciferase Assays. Ten million of EL4 thymoma cells suspended in 500 μl of cold PBS and transfected with 4–20 μg of pcDNA4-NR4A2 or pcDNA4-LacZ in the presence of 10 μg of reporter plasmid, 100 ng of Renilla luciferase plasmid, and 5 μg of DEAE-DEXTRAN (Sigma) by electroporation (250 V, 975 μF, time constant = 30–34 ms) with a GenePulser electroporator II (Bio-Rad). Six hours later, cells were stimulated with 20 ng/ml PMA and 1 μg/ml ionomycin for 24 h, followed by analysis for luciferase activity. The data were normalized for internal controls of Renilla luciferase activity.

Retroviral Infection. Mouse $CD4^+$ T cells purified by AutoMACS using mouse CD4 T isolation kit (Miltenyi Biotec) were stimulated with immobilized anti-CD3 Ab and soluble anti-CD28 Ab in complete medium supplemented with IL-2 (100 units/ml) for 24–48 h before infection. The primed $CD4^+$ T cells were infected twice with retroviruses produced by 293T cells cotransfected with pMIG retroviral vector and pCL-Eco packaging vector. The T cells were cultured in the presence of 30 units/ml of IL-2 for 3 days and were then subjected to intracellular cytokine staining.

Silencing Effects of NR4A2 siRNA on Passive EAE. To evaluate an effect of NR4A2 siRNA, an adoptive transfer EAE model in SJL/J mice was applied, because consistent disease could be induced relatively easily. Female SJL/J mice (8–12 weeks old) (Charles River Laboratories) were immunized s.c. with 100 μg of proteolipid protein (PLP) amino acids 139–151 ($PLP_{139-151}$; HSLGKWLGHPDKF) and 1 mg of heat-killed *M. tuberculosis* H37RA in CFA. Inguinal and popliteal LNs harvested 10 days after immunization were transfected with siRNAs, using hemagglutinating Virus of Japan envelope (HVJ-E) vector kit (GENOMEONE; Ishihara Sangyo). Eight hours later, the cells were stimulated with $PLP_{139-151}$ peptide (35 μg/ml). After 3 days, collected cells were injected i.p. (5×10^6 cells per body) into irradiated mice (3 Gy/body) with intrapelitoneal injection of PT. For conventional histological analysis of EAE, paraffin-embedded spinal cords were stained with either HE or LFB.

Statistics. For statistical analysis, a nonparametric Mann–Whitney *U* test or Student *t* test was used. $P < 0.05$ was considered statistically significant.

Supporting Information. For further details, see *SI Materials and Methods*.

ACKNOWLEDGMENTS. We thank Mayumi Fujita for EAE induction, Miho Mizuno, Chiharu Tomi, and Yuki Kikai for excellent technical assistance. This work was supported by grants from the Ministry of Health, Labour and Welfare of Japan.

1. Sospedra M, Martin R (2005) Immunology of multiple sclerosis. *Annu Rev Immunol* 23:683–747.
2. Hickey WF, Hsu BL, Kimura H (1991) T-lymphocyte entry into the central nervous system. *J Neurosci Res* 28:254–260.
3. Kawakami N, *et al.* (2005) Live imaging of effector cell trafficking and autoantigen recognition within the unfolding autoimmune encephalomyelitis lesion. *J Exp Med* 201:1805–1814.
4. Hur EM, *et al.* (2007) Osteopontin-induced relapse and progression of autoimmune brain disease through enhanced survival of activated T cells. *Nat Immunol* 8:74–83.
5. Gold R, Linington C, Lassmann H (2006) Understanding pathogenesis and therapy of multiple sclerosis via animal models: 70 years of merits and culprits in experimental autoimmune encephalomyelitis research. *Brain* 129:1953–1971.
6. Panitch HS, Hirsch RL, Schindler J, Johnson KP (1987) Treatment of multiple sclerosis with gamma interferon: Exacerbations associated with activation of the immune system. *Neurology* 37:1097–1102.
7. Bielekova B, *et al.* (2000) Encephalitogenic potential of the myelin basic protein peptide (amino acids 83–99) in multiple sclerosis: Results of a phase II clinical trial with an altered peptide ligand. *Nat Med* 6:1167–1175.
8. Willenborg DO, Fordham S, Bernard CC, Cowden WB, Ramshaw IA (1996) IFN-gamma plays a critical down-regulatory role in the induction and effector phase of myelin oligodendrocyte glycoprotein-induced autoimmune encephalomyelitis. *J Immunol* 157:3223–3227.
9. Becher B, Durell BG, Noelle RJ (2002) Experimental autoimmune encephalitis and inflammation in the absence of interleukin-12. *J Clin Invest* 110:493–497.
10. Zhang GX, *et al.* (2003) Induction of experimental autoimmune encephalomyelitis in IL-12 receptor-beta 2-deficient mice: IL-12 responsiveness is not required in the pathogenesis of inflammatory demyelination in the central nervous system. *J Immunol* 170:2153–2160.
11. Cua DJ, *et al.* (2003) Interleukin-23 rather than interleukin-12 is the critical cytokine for autoimmune inflammation of the brain. *Nature* 421:744–748.
12. Langrish CL, *et al.* (2005) IL-23 drives a pathogenic T cell population that induces autoimmune inflammation. *J Exp Med* 201:233–240.
13. Bettelli E, Korn T, Kuchroo VK (2007) Th17: The third member of the effector T cell trilogy. *Curr Opin Immunol* 19:652–657.
14. Lock C, *et al.* (2002) Gene-microarray analysis of multiple sclerosis lesions yields new targets validated in autoimmune encephalomyelitis. *Nat Med* 8:500–508.

15. Tzartos JS, *et al.* (2008) Interleukin-17 production in central nervous system-infiltrating T cells and glial cells is associated with active disease in multiple sclerosis. *Am J Pathol* 172:146–155.
16. Lock CB, Heller RA (2003) Gene microarray analysis of multiple sclerosis lesions. *Trends Mol Med* 9:535–541.
17. Satoh J, *et al.* (2005) Microarray analysis identifies an aberrant expression of apoptosis and DNA damage-regulatory genes in multiple sclerosis. *Neurobiol Dis* 18:537–550.
18. Le WD, *et al.* (2003) Mutations in NR4A2 associated with familial Parkinson disease. *Nat Genet* 33:85–89.
19. Liu ZG, Smith SW, McLaughlin KA, Schwartz LM, Osborne BA (1994) Apoptotic signals delivered through the T-cell receptor of a T-cell hybrid require the immediate-early gene nur77. *Nature* 367:281–284.
20. Woronicz JD, Calnan B, Ngo V, Winoto A (1994) Requirement for the orphan steroid receptor Nur77 in apoptosis of T-cell hybridomas. *Nature* 367:277–281.
21. Cheng LE, Chan FK, Cado D, Winoto A (1997) Functional redundancy of the Nur77 and Nor-1 orphan steroid receptors in T-cell apoptosis. *EMBO J* 16:1865–1875.
22. Calnan BJ, Szychowski S, Chan FK, Cado D, Winoto A (1995) A role for the orphan steroid receptor Nur77 in apoptosis accompanying antigen-induced negative selection. *Immunity* 3:273–282.
23. Satoh J, *et al.* (2006) T cell gene expression profiling identifies distinct subgroups of Japanese multiple sclerosis patients. *J Neuroimmunol* 174:108–118.
24. Maxwell MA, Muscat GE (2006) The NR4A subgroup: Immediate early response genes with pleiotropic physiological roles. *Nucl Recept Signal* 4:e002.
25. Hofstetter HH, Toyka KV, Tary-Lehmann M, Lehmann PV (2007) Kinetics and organ distribution of IL-17-producing CD4 cells in proteolipid protein 139–151 peptide-induced experimental autoimmune encephalomyelitis of SJL mice. *J Immunol* 178:1372–1378.
26. Oki S, Chiba A, Yamamura T, Miyake S (2004) The clinical implication and molecular mechanism of preferential IL-4 production by modified glycolipid-stimulated NKT cells. *J Clin Invest* 113:1631–1640.
27. Meinl E, *et al.* (1993) Myelin basic protein-specific T lymphocyte repertoire in multiple sclerosis. Complexity of the response and dominance of nested epitopes due to recruitment of multiple T cell clones. *J Clin Invest* 92:2633–2643.
28. Inoges S, *et al.* (1999) Cytokine flow cytometry differentiates the clinical status of multiple sclerosis (MS) patients. *Clin Exp Immunol* 115:521–525.
29. Ivanov II, *et al.* (2006) The orphan nuclear receptor RORgammat directs the differentiation program of proinflammatory IL-17+ T helper cells. *Cell* 126:1121–1133.
30. Mucida D, *et al.* (2007) Reciprocal TH17 and regulatory T cell differentiation mediated by retinoic acid. *Science* 317:256–260.
31. Zhou T, *et al.* (1996) Inhibition of Nur77/Nurr1 leads to inefficient clonal deletion of self-reactive T cells. *J Exp Med* 183:1879–1892.
32. Zetterstrom RH, *et al.* (1997) Dopamine neuron agenesis in Nurr1-deficient mice. *Science* 276:248–250.
33. He YW, Deftos ML, Ojala EW, Bevan MJ (1998) RORγ t, a novel isoform of an orphan receptor, negatively regulates Fas ligand expression and IL-2 production in T cells. *Immunity* 9:797–806.
34. Kurebayashi S, *et al.* (2000) Retinoid-related orphan receptor gamma (RORgamma) is essential for lymphoid organogenesis and controls apoptosis during thymopoiesis. *Proc Natl Acad Sci USA* 97:10132–10137.
35. Eberl G, *et al.* (2004) An essential function for the nuclear receptor RORγ(t) in the generation of fetal lymphoid tissue inducer cells. *Nat Immunol* 5:64–73.
36. Bettelli E, *et al.* (2004) Loss of T-bet, but not STAT1, prevents the development of experimental autoimmune encephalomyelitis. *J Exp Med* 200:79–87.
37. Chitnis T, *et al.* (2001) Effect of targeted disruption of STAT4 and STAT6 on the induction of experimental autoimmune encephalomyelitis. *J Clin Invest* 108:739–747.
38. Bettelli E, Oukka M, Kuchroo VK (2007) T(H)-17 cells in the circle of immunity and autoimmunity. *Nat Immunol* 8:345–350.
39. Croxford JL, Miyake S, Huang YY, Shimamura M, Yamamura T (2006) Invariant V(alpha)19i T cells regulate autoimmune inflammation. *Nat Immunol* 7:987–994.

Mol Biol Rep
DOI 10.1007/s11033-008-9330-4

Variation of gene silencing involving endogenous microRNA in mammalian cells

Yoshiko Tamura · Mariko Yoshida · Yusuke Ohnishi · Hirohiko Hohjoh

Received: 22 May 2008 / Accepted: 30 July 2008

Abstract MicroRNAs (miRNAs) are small noncoding RNA and play a role in gene expression regulation by inhibiting translation of their target messenger RNAs (mRNAs). In this study, we investigated the effects of endogenous *let-7* miRNA on the expression of target genes in various mammalian cells by means of two types of reporter plasmids possessing target sequences for *let-7*: one carries perfectly matched target sequence for *let-7* in the 3′-untranslated region of the *luciferase* reporter gene to monitor RNA interference (RNAi) activity and the other has three bulged binding sites for *let-7* to monitor translation-inhibition activity. The results indicate that different cells have different levels of gene silencing against the target reporter genes. The data presented here suggest that not only microRNA level but also target transcript level likely participate in the generation of a variety of gene silencing.

Keywords MicroRNA · *Let-7* · Gene silencing · Variation · Target gene expression

Y. Tamura · M. Yoshida · Y. Ohnishi · H. Hohjoh (✉)
National Institute of Neuroscience, NCNP, 4-1-1 Ogawahigashi, Kodaira, Tokyo 187-8502, Japan
e-mail: hohjohh@ncnp.go.jp

Y. Ohnishi
Department of Human Genetics, Graduate School of Medicine, The University of Tokyo, 7-3-1 Hongo, Bunkyo-ku, Tokyo 113-0033, Japan

Introduction

MicroRNAs (miRNAs) are small noncoding RNA, with a typical length of 19–23 nt, which are processed from longer transcripts by digestion with a microprocessor complex containing Drosha and Pasha in the nucleus and Dicer in the cytoplasm [1–3]. Hundreds of miRNA genes have been found in various species [3–5], and their tissue- or organ-specific expression has been detected [5–7]. After Dicer processing, miRNA duplexes undergo strand selection and then the single-stranded mature miRNA elements are incorporated into the RNA-induced silencing complex (RISC) and function as mediators in suppression of gene expression [8–10]. There are two types of gene silencing involving endogenous miRNAs: one is the inhibition of translation of target mRNAs carrying partially complementary fragments to miRNAs in their 3′ untranslated regions (3′UTRs) [11–15], and the other is the digestion of target RNAs which are perfectly or nearly complementary to miRNAs, such as RNA interference (RNAi) [8, 11, 16]. The gene silencing involving miRNAs play an important role in regulation of gene expression in development, differentiation and proliferation [4, 7, 17–22]. Recent studies have further suggested significant association of miRNAs with various cancers [23–26].

While many findings and data on miRNAs themselves are accumulating, little is known about their target gene expression. It is of interest and importance to realize the entity of regulation of gene expression involving gene silencing mediated by endogenous miRNAs. In this report, we investigated the effects of endogenous *let-7* miRNA on the expression of target genes in various mammalian cells by using reporter plasmids carrying target sequences for *let-7*. The data indicated that different cells had different levels of gene silencing involving endogenous *let-7*.

Materials and methods

Cell culture

Neuro2a (N2a), PC12D, and HeLa cells were grown as previously described [27, 28]. HEK293 cells were grown in Dulbecco's Modified Eagle's Medium (DMEM) (Wako) supplemented with 10% fetal bovine serum (FBS) (Sigma), 100 U/ml penicillin and 100 μg/ml streptomycin (Sigma). F9 cells were grown in DMEM supplemented with 15% FBS and the antibiotics as described above. SH-SY5Y cells were grown in EMEM/F-12 (1:1 mixture) containing 10% FBS and the antibiotics. All the cells were cultured at 37°C in 5% CO_2-humidified chamber. HEK293 (Registry No. JCRB9068) and F9 (Registry No. JCRB0001) cells were purchased from the Health Science Research Resources Bank. SH-SY5Y (Registry No. CRL-2266) cells were purchased from the American Type Culture Collection.

Construction of reporter plasmids

To examine the effects of endogenous *let-7* on gene silencing against its target genes, we constructed reporter plasmids with the psiCHECK-2 plasmid (Promega) carrying the *Renilla* and *Photinus luciferase* genes. The plasmid was digested with *Xho* I and *Pme* I, and subjected to ligation with synthetic oligonucleotide duplexes carrying target sequences for *let-7* (the sequences of the oligonucleotides are indicated below). The resultant plasmids carry perfectly matched target sequence (PMTS) and three bulged binding sites (3xBBS) for *let-7* (Fig. 1). We further constructed reporter plasmids by replacing the Bgl II–Nhe I region containing the simian virus 40 (SV40) promoter in the above plasmids with the Bgl II–Nhe I fragment encoding the herpes simplex virus thymidine kinase (TK) promoter isolated from the phRL-TK plasmid (Promega); the resultant reporter plasmids carry the TK promoter linked with the *Renilla luciferase* gene (Fig. 1).

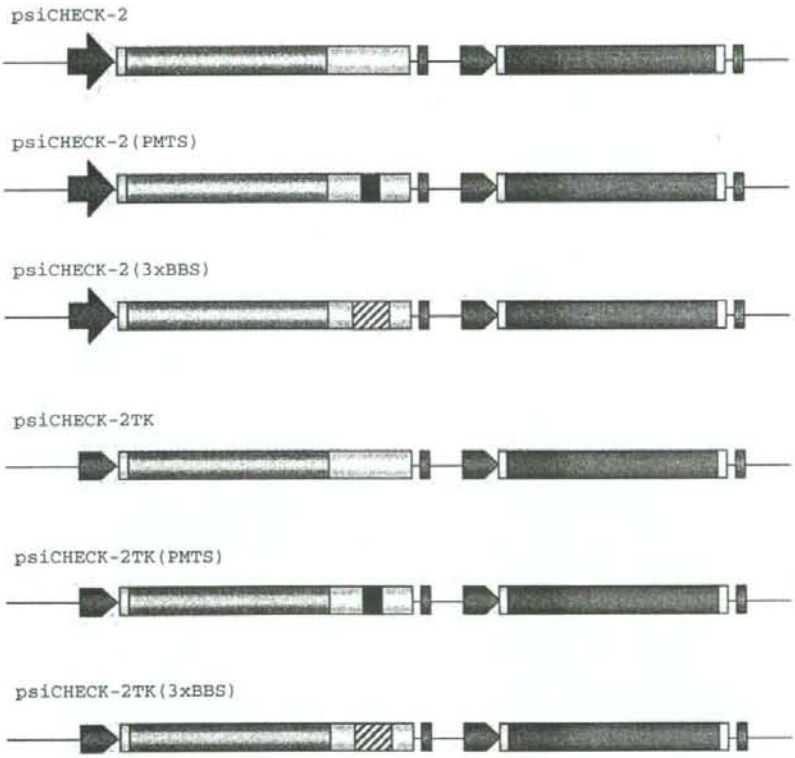

Fig. 1 Constructs of reporter plasmids. Reporter plasmids were constructed based on the psiCHECK-2 plasmid (Promega). Yellow, green, gray and pink boxes indicate the *Renilla* and *Photinus luciferase* coding regions, untranslated region, and poly(A) signal, respectively. Red arrow and orange pentagon indicate the SV40 and TK promoters, respectively. Solid and hatched boxes represent perfectly matched target sequence (PMTS) and three bulged binding sites (3 × BBS) for *let-7*, respectively

The sequences of the oligonucleotides synthesized are as follows:

Ss-let-7(PMTS): 5′-TCGAGAACTATACAACCTACT ACCTCATTACTAGT-3′
As-let-7(PMTS): 5′-ACTAGTAATGAGGTAGTAGGT TGTATAGTTC-3′
Ss-let-7(3 × BBS): 5′-TCGAGGGACAGCCTATTGA ACTACCTCACTCGGAGCACAGCCTATTGAACTAC CTCAGGCCTGCACAGCCTATTGAACTACCTCATT ACTAGT-3′
As-let-7(3 × BBS): 5′-ACTAGTAATGAGGTAGTTC AATAGGCTGTGCAGGCCTGAGGTAGTTCAATAG GCTGTGCTCCGAGTGAGGTAGTTCAATAGGCTGT CCC-3′

Transfection and reporter assay

Transfection of the reporter plasmids was carried out using Lipofectamine 2000 transfection reagent (Invitrogen) according to the manufacturer's instructions, and to each well (24-well culture plates) 0.1 μg of each reporter plasmid was applied. Forty-eight hours after transfection, cell lysate was prepared and the expression levels of luciferases were examined by the Dual-Luciferase reporter assay system (Promega), according to the manufacturer's instructions. The reporter plasmids were also transfected together with either Pre-miR miRNA precursor (Production ID: PM10048; Ambion) or Anti-miR miRNA inhibitor (Production ID: AM10048; Ambion) of *let-7a* into cells, and then the expression of the reporter genes were examined as described above.

Reverse transcription-(real time) polymerase chain reaction (RT-(real time) PCR)

Total RNA was extracted from cells with Trizol reagent (Invitrogen) and subjected to RT-(real time) PCR. Real-time PCR was carried out by means of the AB 7300 Real Time PCR System (Applied Biosystems) with a TaqMan Universal PCR Master Mix together with Assays-on-Demand Gene Expression products (Applied Biosystems) or a SYBR Green PCR Master Mix together with Perfect Real Time Primers (TAKARA BIO), according to the manufacturers' instructions. The Assays-on-Demand Gene Expression products and Perfect Real Time Primers used are shown in Tables 1 and 2, respectively.

To examine the expression levels of *let-7a* and *5sRNA* as a control, total RNA was subjected to RT-PCR using the mirVana qRT-PCR detection kit (Ambion). Real-time PCR was performed by the AB 7300 Real Time PCR system (Applied Biosystems) with SuperTaq polymerase (Ambion). End-point PCR analysis after RT reaction was also carried out by the GeneAmp PCR system 9700 (Applied Biosystems) according to the manufacturer's instructions. The resultant PCR products were electrophoretically separated on 12% polyacrylamide gels and visualized by ethidium bromide staining.

Table 1 Assays-on-demand gene expression products used in this study

Human genes		Mouse genes	
Gene name	Assay ID	Gene name	Assay ID
EIF2C1	Hs00201864_m1	*Eif2c1*	Mm00462977_m1
EIF2C2	Hs00293044_m1	*Eif2c2*	Mm00838341_m1
EIF2C3	Hs00227461_m1	*Eif2c3*	Mm00462959_m1
EIF2C4	Hs00214142_m1	*Eif2c4*	Mm00462659_m1
DICER	Hs00229023_m1	*Zfp36*	Mm00457144_m1
ZFP36	Hs00185658_m1	*Trc6a*	Mm00523487_m1
TRC6A	Hs00379422_m1	*Gapdh*	Mm99999915_g1
GAPDH	Hs99999905_m1		

Table 2 Perfect real time primers used in this study

Human genes		Mouse genes	
Gene name	Primer-Set ID	Gene name	Primer-Set ID
TARBP2	HA039221	*Dicer*	MA043537
PRKRA	HA038462	*Tarbp2*	MA027351
		Prkra	MA030829

DNA chip analysis

Total RNA was extracted from cultured cells using Trizol reagent (Invitrogen). For preparation of cellular miRNAs, small-sized RNAs containing miRNAs were isolated from total RNA using the RNeasy MinElute Cleanup kit (Qiagen). The isolated small-sized RNAs (~1 μg) were subjected to direct labeling with a fluorescent dye using the Platinum*Bright* 647 Infrared nucleic acid labeling kit (KREATECH), according to the manufacturer's instructions. After labeling, the labeled RNAs were purified from free fluorescent substrates by KREA*pure* columns (KREATECH) and used in hybridization. Hybridization was carried out with the *Genopal*®-MICM DNA chips (Mitsubishi Rayon) for detection of mouse miRNAs as described previously [27, 29]. After hybridization, the DNA chips were washed twice in 2 × SSC containing 0.2% SDS at 50°C for 20 min followed by washing in 2 × SSC at 50°C for 10 min, and then hybridization signals were examined and analyzed by means of a DNA chip reader adopting multi-beam excitation technology according to the manufacturer's instructions (Yokogawa Electric Corporation).

Results and discussion

Different cells have different levels of gene silencing mediated by endogenous *let-7*

In order to examine the effects of endogenous miRNAs on the expression of their target genes, we chose the *let-7* miRNA since it had been studied well and because it appeared to be expressed ubiquitously. To investigate the effects of endogenous *let-7* on the expression of its target genes, we performed widely-used assay with luciferase reporter genes carrying target sequences for miRNAs, by which gene silencing with mRNA digestion and translation inhibition mediated by miRNAs can be detected [11, 14, 15, 21, 30–34]. In this study, two types of reporter plasmids were constructed: one carries perfectly matched target sequence (PMTS) for *let-7* in the 3′UTR of the *Renilla luciferase* reporter gene to monitor RNAi activity and the other has three bulged binding sites (3 × BBS) for *let-7* to monitor translation-inhibition activity (Fig. 1), according to the previous studies described by Pillai et al. [14] and Schmitter et al. [34], where the target sequences were shown to undergo distinct gene silencing to each other as described above. The reporter plasmids and empty vector (psiCHECK-2 or psiCHECK-2TK) as a control were transfected into various mammalian cells, and expression of the reporter genes was examined. Figure 2 shows the results. When the target reporter gene carrying PMTS was examined, the expression of the reporter gene (carrying PMTS) was strongly inhibited in the cells except F9 cell, suggesting that potent RNAi activity mediated by endogenous *let-7* occurred in the cells. Interestingly, when the

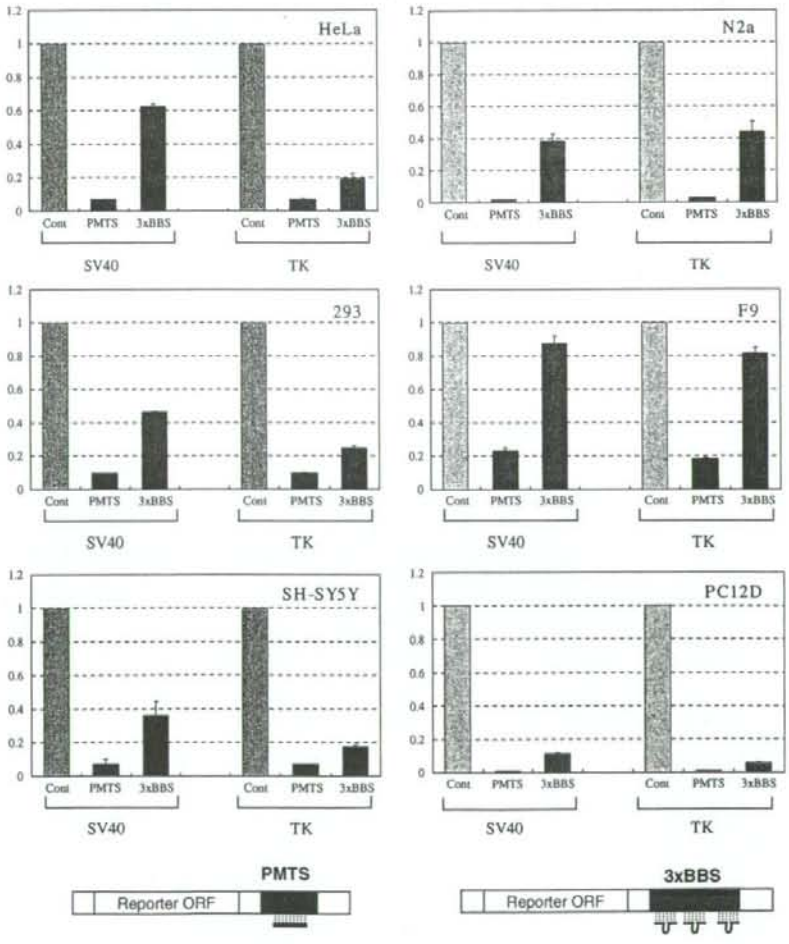

Fig. 2 Knockdown potency of gene silencing mediated by endogenous *let-7*. Reporter genes carrying perfectly matched target sequence (PMTS) and three bulged binding sites (3 × BBS) for *let-7* were constructed (Fig. 1), which are schematically shown together with *let-7* represented by a solid bar or crooked lines. The reporter genes were introduced into indicated cells, and the expression levels of the reporters were examined. Ratios of normalized target (*Renilla*) luciferase activity to control (*Photinus*) luciferase activity are shown: the ratios of luciferase activity in the presence of either PMTS (green bars) or 3 × BBS (pink bars) are normalized to the ratio obtained with the psiCHECK-2 or psiCHECK-2-TK empty plasmid (gray bars) as a control. Data are averages of at least four independent experiments. Error bars represent standard deviations. The SV40 and TK promoters, which drive the reporter genes (Fig. 1), are indicated

reporter gene carrying 3 × BBS was investigated, the level of expression of the target reporter gene varied among the cells, i.e., different cells had different levels of suppression against the target gene. Of the cells investigated, F9 cell exhibited the weakest suppression of the target reporter genes for *let-7*.

Various expression levels of endogenous *let-7* among the cells

In order to address why different cells had different levels of gene silencing (Fig. 2), we investigated the expression of endogenous *let-7* in the cells by means of RT-PCR using specific primers for *let-7a*. As shown in Fig. 3, the results of end-point PCR analyses revealed that the level of *let-7a* varied among the cells: PC12D and SH-SY5Y cells appear to express *let-7a* in a higher level and F9 cell may hardly express it. F9 cell together with N2a cell as a control were further examined by RT-real time PCR followed by analysis with the cycle threshold (Ct) method, and the results suggested that F9 cell might express approximately one-sixth to one-eighth as much *let-7a* as N2a cell (data not shown). We also examined expression profiles of the *let-7* family members by means of the *Genopal*-MICM DNA chips, where DNA probes for the *let-7* members (the mouse *let-7a-g* and *-7i*) are installed. The results of the expression profile analysis indicated that not only *let-7a* but also other *let-7* members were barely present in F9 cell (Fig. 4).

Based on the results, it should be noted that there is a possible correlation between the expression level of *let-7* (Figs. 3, 4) and the suppression level of the target reporter genes (Fig. 2). Data consistent with the possibility were also obtained from experiments with an anti-*let-7* inhibitor: the expression level of the target reporter gene carrying either PMTS or 3 × BBS was increased with an increasing amount of the anti-*let-7* inhibitor, suggesting the reduction of gene silencing mediated by *let-7* with an increasing amount of the anti-*let-7* inhibitor (Fig. 7a). To further

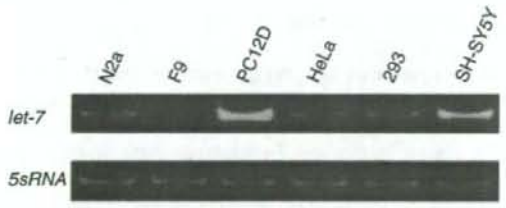

Fig. 3 Expression of endogenous *let-7* in various cells. Total RNA extracted from the indicated cells was subjected to cDNA synthesis, and end-point PCR analysis of *let-7* and *5sRNA* as a control was carried out. The resultant PCR products were examined by electrophoresis with 12% polyacrylamide gels followed by ethidium bromide staining

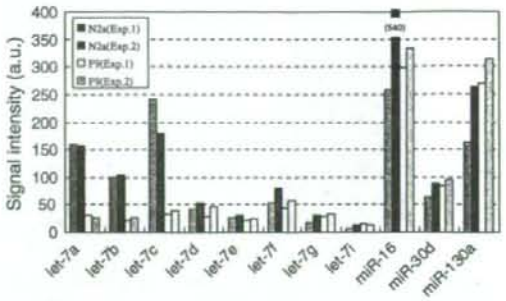

Fig. 4 Expression profiles of *let-7* miRNAs. Small-sized RNAs extracted from F9 and N2a cells were examined by the *Genopal*®-MICM DNA chips (Mitsubishi Rayon). Expression profiles of *let-7* members (indicated) and miR-16, −30d and −130a as positive controls are shown. Hybridization signal intensity of each miRNA was subjected to background subtraction and indicated by arbitrary intensity units (a.u.). The intensity which is over the plotted area is indicated in a parenthesis. Expression profile analysis was repeated individually (Exps. 1 and 2)

evaluate the possibility, we examined the expression of genes associated with RNAi and/or miRNA pathways. The *Ago1-4*, *Dicer*, *Pact*, *Tarbp2*, *Zfp36*, and *Trc6a* genes were investigated by RT-real time PCR (Fig. 5), and the results indicated that the expression profiles of the genes were similar among the cells, suggesting little correlation of the expression of the genes with various suppression levels of the target reporter genes.

Since F9 cell exhibited weak suppression against the target reporter genes for *let-7* (Fig. 2), we examined whether the cell possessed immature gene silencing machinery

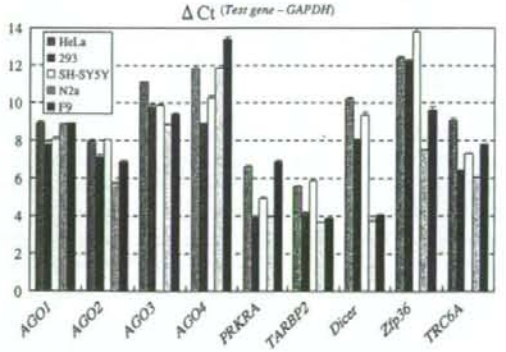

Fig. 5 Expression profiles of genes involved in gene silencing pathways. Total RNA was extracted from indicated cells and examined by RT-real time PCR. The genes examined are indicated. Expression levels of the genes were analyzed by the cycle threshold (Ct) method: the difference between their Ct and the Ct of the *Gapdh* gene examined as a control [$\Delta Ct^{(Test\ gene\ -\ Gapdh)}$] was calculated and plotted. Data are averages of three measurements by RT-real time PCR analyses. Error bars represent standard deviations

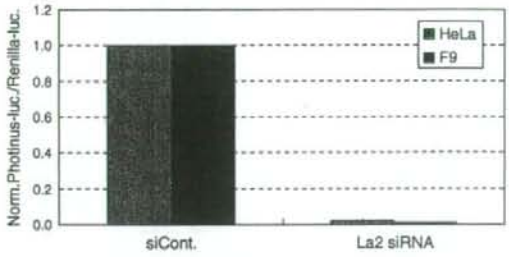

Fig. 6 RNAi activities induced by synthetic siRNA duplex in F9 cells. Chemically synthesized La2 siRNA duplex against the *Photinus luciferase* gene [35] together with pGL3-control (Promega) and phRL-TK plasmids (Promega) carrying *Photinus* and *Renilla luciferase* reporter genes, respectively, were cotransfected into F9 and HeLa (control) cells. Twenty-four hours after transfection, cell lysate was prepared, and dual-luciferase assay was carried out and analyzed as described previously [35]. Data are averages of at least three independent experiments. Error bars represent standard deviations

by using an exogenous (chemically synthesized) siRNA duplex triggering strong RNAi. The La2 siRNA duplex, which can induce strong RNAi activity against the *Photinus luciferase* gene [35], was cotransfected with the target reporter gene into F9 cells. As shown in Fig. 6, consistent with the previous results [35, 36], the cells exhibited potent RNAi, suggesting that F9 cell possesses a full-RNAi machinery. This has been also supported by experiments with a synthetic pre-*let-7* precursor: the expression level of the target reporter gene carrying either PMTS or 3 × BBS was decreased in the presence of the pre-*let-7* precursor (Fig. 7b). Taken together, the data presented here suggest that the expression level of *let-7* greatly influences the level of gene silencing against its target genes.

Effect of transcriptional activity of target gene on gene silencing

In this study, we also examined the effect of transcriptional activity of the target reporter genes on gene silencing. The SV40 and TK promoters, which drive the reporter genes (Fig. 1), appear to have different promoter activities: the transcriptional activity of the SV40 promoter appears to be stronger than that of the TK promoter in the cells examined here (Fig. 8). When suppression level was examined between the promoters, little or no difference in suppression of the reporter gene carrying PMTS was detected, and in contrast, the reporter gene carrying 3 × BBS appeared to exhibit difference in suppression level between the promoters. Table 3 shows relative expression level of the target reporter gene carrying 3 × BBS, when the expression level of the target gene carrying PMTS is given as 1; and the data indicate differences in the relative expression levels between the promoters. Taken together, it is suggested that

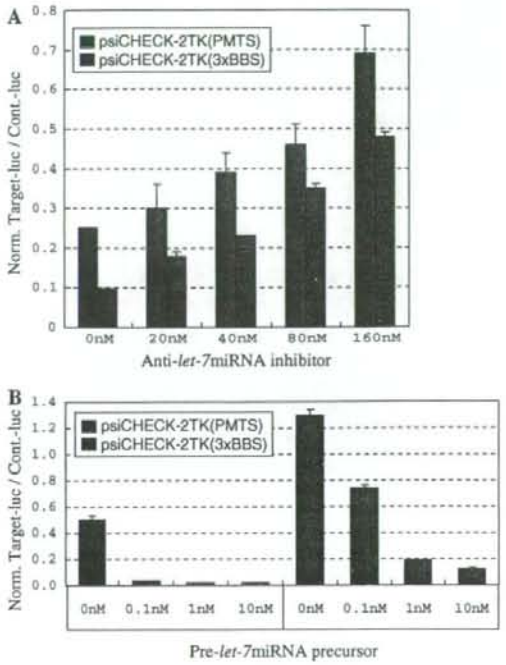

Fig. 7 Dose-dependent suppression of target reporter genes. The psiCHECK-2-TK(PMTS) and psiCHECK-2-TK(3 × BBS) plasmids were cotransfected with an increasing amount of the Anti-miR miRNA inhibitor of *let-7a* (Ambion), from 0 to 160 nM, into 293 cells (**a**), or an increasing amount of the Pre-miR miRNA precursor of *let-7a* (Ambion), from 0 to 20 nM, into F9 cells (**b**). 48 and 24 h after transfection with the inhibitor and precursor, respectively, cell extract was prepared and dual-luciferase assay was carried out. Data are presented as normalized ratios of target (*Renilla*) luciferase activity to control (*Photinus*) luciferase activity as in Fig. 2

different expression levels of one particular target gene undergoing gene silencing by translation inhibition may be reflected in a variety of its gene expression, whereas those undergoing gene silencing by RNAi may be not.

Variety of gene silencing

The data presented here suggest possible parameters conferring a variety of gene silencing: (i) level of endogenous miRNA and (ii) level of target mRNA. In addition, it has been known that various base-pairing interactions can be formed between miRNAs and their target mRNAs [31, 37]. It is conceivable that these parameters presumably raise a great deal of combination between miRNAs and target mRNAs in a qualitative and quantitative manner. Accordingly, the resultant gene silencing based on such a combination may yield various levels of suppression against target mRNAs, thereby conferring a variety of gene expression.

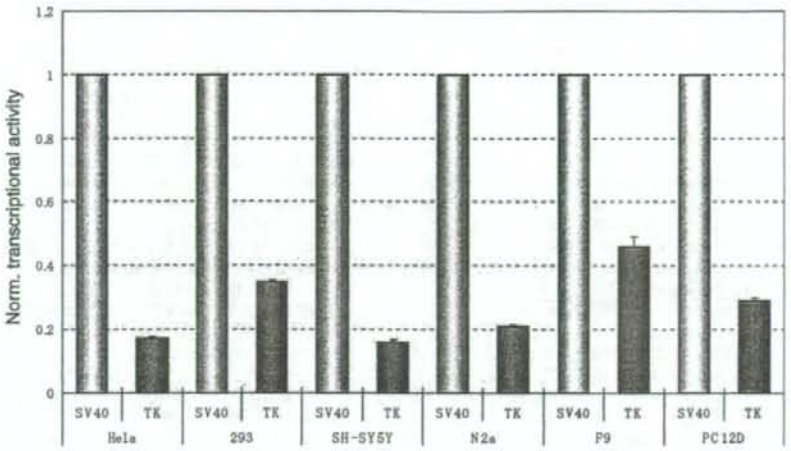

Fig. 8 Transcriptional activity. The transcriptional activities of the SV40 and TK promoters which drive the target reporter (*Renilla luciferase*) gene were investigated in the cells (indicated). The psiCHECK-2 and psiCHECK-2-TK empty plasmids were introduced into the cells and the expressed luciferases were examined as in Fig. 2. Ratios of normalized *Renilla* luciferase activity to control *Photinus* luciferase activity are shown: the ratio of the *Renilla* luciferase activity in the presence of psiCHECK-2-TK is normalized to the ratio obtained in the presence of psiCHECK-2 in each cell. Data are averages of at least three independent experiments. Error bars represent standard deviations

Table 3 Relative expression levels of target reporter gene carrying 3 × BBS

Cell name	SV40[a]	TK[a]
HeLa	9.09	2.85
293	4.84	2.53
SH-SY5Y	5.12	2.57
N2a	21.7	16.3
F9	3.76	4.44
PC12D	11.4	6.1

The relative expression level is indicated when the expression level of the target reporter gene carrying PMTS is given as 1 under each promoter

[a] Used promoters for driving the target reporter genes

Acknowledgements We would like to thank T. Fukushima (Mitsubishi Rayon) for his helpful assistance. This work was supported in part by research grants from the Ministry of Health, Labour and Welfare of Japan and by Grants-in-Aid for Scientific Research from the Japan Society for the Promotion of Science.

References

1. Lee Y, Ahn C, Han J et al (2003) The nuclear RNase III Drosha initiates microRNA processing. Nature 425:415–419. doi:10.1038/nature01957
2. Denli AM, Tops BB, Plasterk RH et al (2004) Processing of primary microRNAs by the Microprocessor complex. Nature 432:231–235. doi:10.1038/nature03049
3. Bartel DP (2004) MicroRNAs: genomics, biogenesis, mechanism, and function. Cell 116:281–297. doi:10.1016/S0092-8674(04)00045-5
4. Krichevsky AM, King KS, Donahue CP et al (2003) A microRNA array reveals extensive regulation of microRNAs during brain development. RNA 9:1274–1281. doi:10.1261/rna.5980303
5. Lagos-Quintana M, Rauhut R, Yalcin A et al (2002) Identification of tissue-specific microRNAs from mouse. Curr Biol 12:735–739. doi:10.1016/S0960-9822(02)00809-6
6. Babak T, Zhang W, Morris Q et al (2004) Probing microRNAs with microarrays: tissue specificity and functional inference. RNA 10:1813–1819. doi:10.1261/rna.7119904
7. Liu CG, Calin GA, Meloon B et al (2004) An oligonucleotide microchip for genome-wide microRNA profiling in human and mouse tissues. Proc Natl Acad Sci USA 101:9740–9744. doi:10.1073/pnas.0403293101
8. Hutvagner G, Zamore PD (2002) A microRNA in a multiple-turnover RNAi enzyme complex. Science 297:2056–2060. doi:10.1126/science.1073827
9. Caudy AA, Myers M, Hannon GJ et al (2002) Fragile X-related protein and VIG associate with the RNA interference machinery. Genes Dev 16:2491–2496. doi:10.1101/gad.1025202
10. Schwarz DS, Hutvagner G, Du T et al (2003) Asymmetry in the assembly of the RNAi enzyme complex. Cell 115:199–208. doi:10.1016/S0092-8674(03)00759-1
11. Zeng Y, Yi R, Cullen BR (2003) MicroRNAs and small interfering RNAs can inhibit mRNA expression by similar mechanisms. Proc Natl Acad Sci USA 100:9779–9784. doi:10.1073/pnas.1630797100
12. Olsen PH, Ambros V (1999) The lin-4 regulatory RNA controls developmental timing in Caenorhabditis elegans by blocking LIN-14 protein synthesis after the initiation of translation. Dev Biol 216:671–680. doi:10.1006/dbio.1999.9523
13. Liu J, Valencia-Sanchez MA, Hannon GJ et al (2005) MicroRNA-dependent localization of targeted mRNAs to mammalian P-bodies. Nat Cell Biol 7:719–723. doi:10.1038/ncb1274
14. Pillai RS, Bhattacharyya SN, Artus CG et al (2005) Inhibition of translational initiation by Let-7 MicroRNA in human cells. Science 309:1573–1576. doi:10.1126/science.1115079

15. Doench JG, Petersen CP, Sharp PA (2003) siRNAs can function as miRNAs. Genes Dev 17:438–442. doi:10.1101/gad.1064703
16. Yekta S, Shih IH, Bartel DP (2004) MicroRNA-directed cleavage of HOXB8 mRNA. Science 304:594–596. doi:10.1126/science.1097434
17. Chen CZ, Li L, Lodish HF et al (2004) MicroRNAs modulate hematopoietic lineage differentiation. Science 303:83–86. doi:10.1126/science.1091903
18. Chen JF, Mandel EM, Thomson JM et al (2006) The role of microRNA-1 and microRNA-133 in skeletal muscle proliferation and differentiation. Nat Genet 38:228–233. doi:10.1038/ng1725
19. Schratt GM, Tuebing F, Nigh EA et al (2006) A brain-specific microRNA regulates dendritic spine development. Nature 439:283–289. doi:10.1038/nature04367
20. Zhao Y, Samal E, Srivastava D (2005) Serum response factor regulates a muscle-specific microRNA that targets Hand2 during cardiogenesis. Nature 436:214–220. doi:10.1038/nature03817
21. Cheng AM, Byrom MW, Shelton J et al (2005) Antisense inhibition of human miRNAs and indications for an involvement of miRNA in cell growth and apoptosis. Nucleic Acids Res 33:1290–1297. doi:10.1093/nar/gki200
22. Hornstein E, Mansfield JH, Yekta S et al (2005) The microRNA miR-196 acts upstream of Hoxb8 and Shh in limb development. Nature 438:671–674. doi:10.1038/nature04138
23. Calin GA, Dumitru CD, Shimizu M et al (2002) Frequent deletions and down-regulation of micro-RNA genes miR15 and miR16 at 13q14 in chronic lymphocytic leukemia. Proc Natl Acad Sci USA 99:15524–15529. doi:10.1073/pnas.242606799
24. Eis PS, Tam W, Sun L et al (2005) Accumulation of miR-155 and BIC RNA in human B cell lymphomas. Proc Natl Acad Sci USA 102:3627–3632. doi:10.1073/pnas.0500613102
25. He L, Thomson JM, Hemann MT et al (2005) A microRNA polycistron as a potential human oncogene. Nature 435:828–833. doi:10.1038/nature03552
26. Johnson SM, Grosshans H, Shingara J et al (2005) RAS is regulated by the let-7 microRNA family. Cell 120:635–647. doi:10.1016/j.cell.2005.01.014
27. Hohjoh H, Fukushima T (2007) Marked change in microRNA expression during neuronal differentiation of human teratocarcinoma NTera2D1 and mouse embryonal carcinoma P19 cells. Biochem Biophys Res Commun 362:360–367. doi:10.1016/j.bbrc.2007.07.189
28. Ohnishi Y, Tokunaga K, Kaneko K, Hohjoh H (2006) Assessment of allele-specific gene silencing by RNA interference with mutant and wild-type reporter alleles. J RNAi Gene Silencing 2:154–160
29. Hohjoh H, Fukushima T (2007) Expression profile analysis of microRNA (miRNA) in mouse central nervous system using a new miRNA detection system that examines hybridization signals at every step of washing. Gene 391:39–44. doi:10.1016/j.gene.2006.11.018
30. Kiriakidou M, Nelson PT, Kouranov A et al (2004) A combined computational-experimental approach predicts human microRNA targets. Genes Dev 18:1165–1178. doi:10.1101/gad.1184704
31. Lewis BP, Shih IH, Jones-Rhoades MW et al (2003) Prediction of mammalian microRNA targets. Cell 115:787–798. doi:10.1016/S0092-8674(03)01018-3
32. O'Donnell KA, Wentzel EA, Zeller KI et al (2005) c-Myc-regulated microRNAs modulate E2F1 expression. Nature 435:839–843. doi:10.1038/nature03677
33. Petersen CP, Bordeleau ME, Pelletier J et al (2006) Short RNAs repress translation after initiation in mammalian cells. Mol Cell 21:533–542. doi:10.1016/j.molcel.2006.01.031
34. Schmitter D, Filkowski J, Sewer A et al (2006) Effects of Dicer and Argonaute down-regulation on mRNA levels in human HEK293 cells. Nucleic Acids Res 34:4801–4815. doi:10.1093/nar/gkl646
35. Hohjoh H (2002) RNA interference (RNAi) induction with various types of synthetic oligonucleotide duplexes in cultured human cells. FEBS Lett 521:195–199. doi:10.1016/S0014-5793(02)02860-0
36. Sago N, Omi K, Tamura Y et al (2004) RNAi induction and activation in mammalian muscle cells where Dicer and eIF2C translation initiation factors are barely expressed. Biochem Biophys Res Commun 319:50–57. doi:10.1016/j.bbrc.2004.04.151
37. Lewis BP, Burge CB, Bartel DP (2005) Conserved seed pairing, often flanked by adenosines, indicates that thousands of human genes are microRNA targets. Cell 120:15–20. doi:10.1016/j.cell.2004.12.035

THE JOURNAL OF BIOLOGICAL CHEMISTRY VOL. 283, NO. 35, pp. 23731–23738, August 29, 2008

Aberrant Interaction between Parkinson Disease-associated Mutant UCH-L1 and the Lysosomal Receptor for Chaperone-mediated Autophagy*[S]

Received for publication, March 10, 2008, and in revised form, June 12, 2008 Published, JBC Papers in Press, June 12, 2008, DOI 10.1074/jbc.M801918200

Tomohiro Kabuta[‡1], Akiko Furuta[‡], Shunsuke Aoki[‡2], Koh Furuta[§], and Keiji Wada[‡3]

From the [‡]Department of Degenerative Neurological Diseases, National Institute of Neuroscience, National Center of Neurology and Psychiatry, 4-1-1 Ogawahigashi, Kodaira, Tokyo 187-8502, Japan and the [§]Division of Clinical Laboratories, National Cancer Center Hospital, 5-1-1 Tsukiji, Chuo-ku, Tokyo 104-0045, Japan

Parkinson disease (PD) is the most common neurodegenerative movement disorder. An increase in the amount of α-synuclein protein could constitute a cause of PD. α-Synuclein is degraded at least partly by chaperone-mediated autophagy (CMA). The I93M mutation in ubiquitin C-terminal hydrolase L1 (UCH-L1) is associated with familial PD. However, the relationship between α-synuclein and UCH-L1 in the pathogenesis of PD has remained largely unclear. In this study, we found that UCH-L1 physically interacts with LAMP-2A, the lysosomal receptor for CMA, and Hsc70 and Hsp90, which can function as components of the CMA pathway. These interactions were abnormally enhanced by the I93M mutation and were independent of the monoubiquitin binding of UCH-L1. In a cell-free system, UCH-L1 directly interacted with the cytosolic region of LAMP-2A. Expression of I93M UCH-L1 in cells induced the CMA inhibition-associated increase in the amount of α-synuclein. Our findings may provide novel insights into the molecular links between α-synuclein and UCH-L1 and suggest that aberrant interaction of mutant UCH-L1 with CMA machinery, at least partly, underlies the pathogenesis of PD associated with I93M UCH-L1.

Parkinson disease (PD)[4] is the most common neurodegenerative movement disorder characterized by progressive degeneration confined mostly to dopaminergic neurons in the substantia nigra pars compacta. Although the majority of PD cases occur sporadically, nine genes have been reported to be associated with familial forms of PD. Several missense mutations in the α-synuclein gene are linked to dominantly inherited PD (1–3). Duplication and triplication of the α-synuclein gene were also shown to cause familial PD or parkinsonism (4–6), indicating that increases in the levels of α-synuclein could constitute a cause of PD. α-Synuclein is a major component of cytoplasmic inclusions called Lewy bodies in the brains of patients with sporadic PD (7, 8). These findings raised the idea that α-synuclein plays a central role in the pathogenesis of PD. Therefore, elucidating the molecular relationships between α-synuclein and other familial PD-associated proteins is important for understanding the mechanisms that underlie the pathology of PD.

A missense mutation in the ubiquitin C-terminal hydrolase L1 (UCH-L1) gene, leading to an I93M substitution at the protein level, has been reported in two affected siblings of a German family with dominantly inherited PD (9). In this family, four of seven family members were affected with PD. However, the family members, except the two siblings, were not genotyped. There was an unaffected presumed carrier of the I93M mutation in the family. Therefore, the link between the I93M mutation and the development of PD has been questioned (10, 11). To clarify the link between the mutation and PD, we have generated UCH-L1^{I93M} transgenic mice and reported that these mice exhibit progressive dopaminergic cell loss (12). In addition, we have shown that, compared with UCH-L1^{WT}, UCH-L1^{I93M} exhibits increased insolubility and levels of interactions with other proteins in mammalian cells, features that are characteristic of several neurodegenerative disease-linked mutants (13). These findings suggest that the I93M mutation in UCH-L1 contributes to the pathogenesis of PD. UCH-L1 has also been identified as a component of several inclusion bodies characteristic of neurodegenerative diseases including Lewy bodies (14). A polymorphism in the UCH-L1 gene, resulting in an S18Y substitution at the amino acid residue level, has been reported to be associated with decreased risk of PD in certain populations but not in other populations (15, 16). We have also reported that UCH-L1^{I93M} and carbonyl-modified UCH-L1, which is associated with sporadic PD (17), display shared aberrant properties (13), suggesting that carbonyl-modified UCH-L1 constitutes one of the causes of sporadic PD.

* This work was supported by grants-in-aid for scientific research from the Japan Society for the Promotion of Science; a research grant in priority area research from the Ministry of Education, Culture, Sports, Science, and Technology, Japan; grants-in-aid for scientific research from the Ministry of Health, Labor, and Welfare, Japan; and the Program for Promotion of Fundamental Studies in Health Sciences of the National Institute of Biomedical Innovation and the New Energy and Industrial Technology Development Organization, Japan. The costs of publication of this article were defrayed in part by the payment of page charges. This article must therefore be hereby marked "*advertisement*" in accordance with 18 U.S.C. Section 1734 solely to indicate this fact.

[S] The on-line version of this article (available at http://www.jbc.org) contains supplemental "Experimental Procedures," Figs. S1 and S2, and an additional reference.

[1] To whom correspondence may be addressed. Tel.: 81-42-346-1715; Fax: 81-42-346-1745; E-mail: kabuta@ncnp.go.jp.

[2] Present address: Dept. of Bioscience and Bioinformatics, Kyushu Inst. of Technology, 680-4 Kawazu, Iizuka-shi, Fukuoka 820-8502, Japan.

[3] To whom correspondence may be addressed. Tel.: 81-42-346-1715; Fax: 81-42-346-1745; E-mail: wada@ncnp.go.jp.

[4] The abbreviations used are: PD, Parkinson disease; UCH-L1, ubiquitin C-terminal hydrolase L1; WT, wild-type; CMA, chaperone-mediated autophagy; LAMP-2, lysosome-associated membrane protein type 2; Hsc70, heat shock cognate protein 70; Hsp90, heat shock protein 90; GAPDH, glyceraldehyde-3-phosphate dehydrogenase.

UCH-L1 is one of the most abundant proteins in the brain (1–5% of total soluble protein) (18) and is thought to hydrolyze ubiquitin conjugates into monoubiquitin (19). UCH-L1 was also reported to function as a ubiquitin ligase for monoubiquitinated α-synuclein in a cell-free system (20). Other than these enzymatic activities, we have reported that UCH-L1 stabilizes monoubiquitin by binding to monoubiquitin in neurons (21). Although the hydrolase activity of UCH-L1^{I93M} and the binding of UCH-L1^{I93M} to monoubiquitin are decreased compared with those of UCH-L1^{WT} (9, 13, 22), we have shown that mice deficient in UCH-L1 do not display obvious dopaminergic cell loss (21, 23). These observations indicate that the main cause of UCH-L1^{I93M}-associated PD may not be a loss of UCH-L1 function but an acquired toxicity of UCH-L1^{I93M}. Our previous studies also suggest that aberrantly enhanced physical interactions between UCH-L1^{I93M} and multiple proteins, including tubulin, underlie the toxic functions of UCH-L1^{I93M} (13).

However, the molecular relationship between α-synuclein and UCH-L1 in the pathogenesis of PD has remained largely unclear. α-Synuclein is known to be degraded at least partly by chaperone-mediated autophagy (CMA) (24), in which substrate proteins are selectively transported to and degraded in lysosomes (25). In this study, we sought to identify novel UCH-L1-interacting proteins. We found that UCH-L1 physically interacts with lysosome-associated membrane protein type 2A (LAMP-2A), heat shock cognate protein 70 (Hsc70), and heat shock protein 90 (Hsp90), all of which are components of the CMA pathway (26). These interactions were enhanced by the I93M mutation in UCH-L1 and were independent of the interaction between monoubiquitin and UCH-L1. We also provide the data suggesting that the aberrant interaction of UCH-L1 with CMA machinery results in the accumulation of α-synuclein.

EXPERIMENTAL PROCEDURES

Plasmids—pCI-neo-hUCH-L1 plasmids containing human WT UCH-L1 and UCH-L1 variants with or without a FLAG tag were prepared as described previously (13). The regulatory expression plasmids pTRE-Tight-hUCH-L1 containing WT and I93M UCH-L1 with a FLAG tag at the C terminus of UCH-L1 were constructed by ligating the cDNA encoding UCH-L1 into the pTRE-Tight (Clontech) vector. The expression plasmid pCI-neo-hα-synuclein was constructed using the pCI-neo mammalian expression vector (Promega), and the expression plasmid pCI-neo-ΔDQ α-synuclein was generated using a QuikChange site-directed mutagenesis kit (Stratagene).

Cell Culture and Transfection—COS-7 cells were maintained in Dulbecco's modified Eagle's medium (Sigma) supplemented with 10% fetal bovine serum (JRH Biosciences, Lenexa, KS). IMR-90 cells, which have been used to study CMA (27), were cultured as described in the literature (27). NIH-3T3 cells stably expressing human UCH-L1 with a FLAG-hemagglutinin double tag at the N terminus were cultured as described previously (13). Transient transfection of COS-7 and IMR-90 cells with each vector was performed using Lipofectamine reagent (Invitrogen) and Lipofectamine LTX reagent (Invitrogen), respectively. There was no notable difference in the transfection efficiency among the culture dishes (wells) in our experimental conditions (data not shown).

Immunoblotting and Immunoprecipitation—Preparation of the detergent (1% Triton X-100)-soluble fraction was performed as described previously (28). The cytosolic fraction that does not contain LAMP-2, a marker of lysosomes, and the crude lysosomal fraction containing LAMP-2 (supplemental Fig. S1*A*) were prepared according to the method described by Pertoft *et al.* (29). SDS-PAGE was performed under reducing conditions. Immunoblotting was performed according to standard procedures as described previously (30). For some experiments, Can Get Signal Immunoreaction Enhancer Solution (Toyobo, Osaka, Japan) was used. The signal intensity was quantified by densitometry using FluorChem software (Alpha Innotech, San Leandro, CA). Immunoprecipitation was performed using anti-FLAG M2 affinity gel (Sigma) or 10 μg/ml antibodies (unless otherwise mentioned) with protein G-Sepharose (GE Healthcare), as described previously (13). The antibodies used were as follows. Antibodies against UCH-L1, Cu,Zn-superoxide dismutase 1, Hsc70, and Hsp90 were purchased from Ultra-Clone, Stressgen Bioreagents (Victoria, Canada), Affinity BioReagents (Golden, CO), and BD Transduction Laboratories (Franklin Lakes, NJ), respectively. Anti-β-actin, Mcl-1, and FLAG antibodies were from Sigma. Antibodies against α-synuclein and glyceraldehyde-3-phosphate dehydrogenase (GAPDH) were from Chemicon (Temecula, CA). Anti-p53 and Bcl-xL antibodies were from Cell Signaling. Anti-Bcl-2, Ubc9, NF-κB p65, and LAMP-2 antibodies were from Santa Cruz Biotechnology. The rabbit polyclonal anti-LAMP-2A antibody was raised in rabbit against a synthetic peptide (CYFIGLKHHHAGYEQF) containing an amino acid sequence corresponding to the cytosolic region of human LAMP-2A. The specificity of the anti-LAMP-2A antibody was confirmed as shown in supplemental Fig. S1, *B* and *C*.

Pulldown Assay—Recombinant human UCH-L1 proteins without a tag were prepared as described previously (13). A pulldown assay was performed as described previously (13) with slight modifications. Streptavidin-Sepharose (GE Healthcare) was blocked with 3% bovine serum albumin for 15 h to prevent nonspecific binding of UCH-L1 to the beads and washed three times with phosphate-buffered saline containing 0.05% Triton X-100. Ten μg of UCH-L1 (wild-type or I93M) and 2 nmol of synthetic peptides conjugated to biotin (control or LAMP-2A peptide, Invitrogen) were mixed and incubated for 15 h in phosphate-buffered saline containing 0.05% Triton X-100. Twenty μl of streptavidin beads blocked with bovine serum albumin was then added, and incubation was continued for 1 h. After beads were washed three times with phosphate-buffered saline containing 0.05% Triton X-100, proteins were eluted with SDS sample buffer and subjected to SDS-PAGE.

UCH-L1 Degradation Assay—COS-7 cells were cotransfected with pTet-Off and pTRE-Tight-hUCH-L1. Twenty-four h after transfection, transcription of UCH-L1-FLAG gene was suppressed by adding 100 ng/ml doxycycline and incubating for 4 h. Then, cells were harvested at the 0-, 24-, and 48-h time

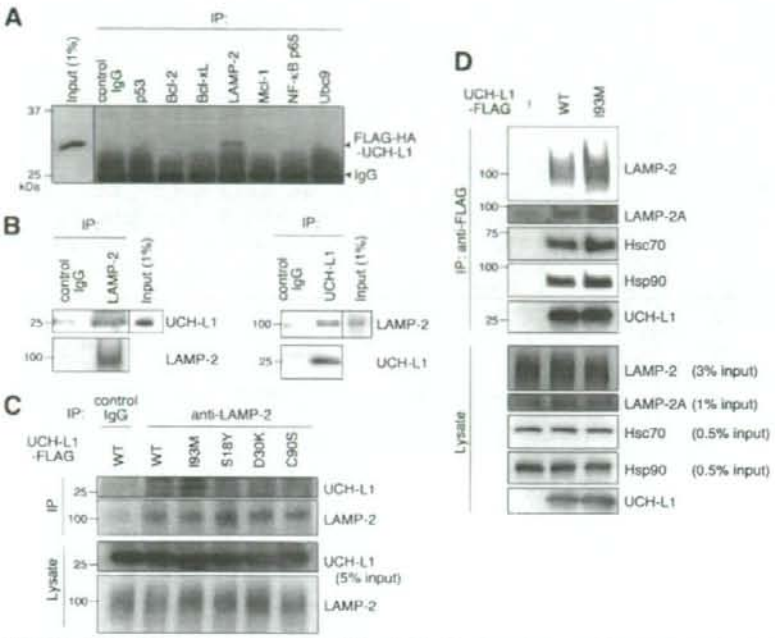

FIGURE 1. **Physical interactions of UCH-L1 with LAMP-2A, Hsc70, and Hsp90.** *A*, lysates of NIH-3T3 cells stably expressing FLAG-hemagglutinin (*HA*)-tagged UCH-L1 were immunoprecipitated (*IP*) with antibodies against cell death- or protein degradation-related proteins and analyzed by immunoblotting using anti-UCH-L1 antibody. A representative blot including immunoprecipitant with anti-LAMP-2 antibody is shown. *B*, mouse (C57BL/6J) whole brain lysates were immunoprecipitated with control IgG, anti-LAMP-2, or anti-UCH-L1 antibody and immunoblotted with anti-UCH-L1 and LAMP-2 antibodies. *C*, lysates of COS-7 cells transfected with the indicated constructs were immunoprecipitated with 5 μg/ml control IgG or anti-LAMP-2 antibody and analyzed by immunoblotting using anti-UCH-L1 antibody. *D*, lysates of COS-7 cells transfected with the indicated constructs (−, empty vector) were immunoprecipitated with anti-FLAG beads and immunoblotted using anti-LAMP2, LAMP-2A, Hsc70, Hsp90, and UCH-L1 antibodies.

points after the suppression of the gene and analyzed by immunoblotting. Pulse-chase analyses were performed as described previously (21) with some modifications. COS-7 cells transfected with pCI-neo-hUCH-L1-FLAG were washed and incubated with methionine-, cysteine-, and cystine-free medium for 1 h. The cells were pulsed with 0.1 mCi/ml [^{35}S]Met and [^{35}S]Cys (Expre^{35}S^{35}S protein labeling mixture, PerkinElmer Life Sciences) for 1 h and then washed and chased with 3 mM methionine and cysteine for 48 h. At the 0-, 24-, and 48-h time points, the cells were harvested for immunoprecipitation with anti-FLAG M2 affinity gel. Following SDS-PAGE on a 15% gel, radioactive bands were detected and analyzed by using a BAS-5000 imaging analyzer (Fujifilm, Tokyo, Japan).

Statistical Analysis—For comparison of two groups, the statistical significance of differences was determined by the Student's *t* test.

RESULTS

UCH-L1 Interacts with LAMP-2A, Hsc70, and Hsp90—We have previously shown that soluble UCH-L1 interacts with multiple proteins in mammalian cells and that one of the UCH-L1-interacting proteins is α/β-tubulin (13). In this study, we further screened for UCH-L1-interacting proteins using a coimmunoprecipitation assay (Fig. 1*A*). We identified LAMP-2 as a novel UCH-L1-interacting protein (Fig. 1*A*). To confirm this interaction *in vivo*, a coimmunoprecipitation assay was performed using mouse whole brain lysate. Interaction between endogenous UCH-L1 and endogenous LAMP-2 was observed (Fig. 1*B*). LAMP-2 exists in three different isoforms, LAMP-2A, LAMP-2B, and LAMP-2C, which are produced by the alternative splicing of the LAMP-2 pre-mRNA (31). LAMP-2A forms a complex with chaperones such as Hsc70 and Hsp90 and functions as a receptor for CMA at the lysosomal membrane (26). Because α-synuclein has been reported to interact with LAMP-2A (24), we tested for interactions between UCH-L1 and LAMP-2A, Hsc70, and Hsp90. The UCH-L1 immunoprecipitant included LAMP-2A as well as Hsc70 and Hsp90 (Fig. 1*D*). These results indicate that UCH-L1 interacts with LAMP-2A, Hsc70, and Hsp90 in mammalian cells.

UCH-L1 Can Be Degraded by Macroautophagy—Although UCH-L1 physically interacts with LAMP-2A, UCH-L1 is not a presumable substrate for CMA because UCH-L1 does not contain a KFERQ-like motif, which is required for substrate proteins to be degraded by CMA (32). Therefore, we speculated that UCH-L1 is degraded by other degradation pathways in mammalian cells. We used a regulatory protein expression system to switch off the expression of UCH-L1 by adding doxycycline, to follow UCH-L1 degradation. Degradation of UCH-L1 was observed 24 or 48 h after expression was switched off, compared with the time point at which expression was switched off (Fig. 2*A*). The half-life of UCH-L1 was >48 h (Fig. 2*A*). Long-lived proteins are known to be mainly degraded by macroautophagy (33). We therefore investigated whether UCH-L1 was degraded by macroautophagy using 3-MA, an inhibitor of macroautophagy (24, 28, 34). The 3-MA treatment significantly inhibited the degradation of UCH-L1 (Fig. 2*A*). Similar results were obtained when we used UCH-L1^{I93M} (Fig. 2*B*). Pulse-chase experiments also showed that the degradations of UCH-L1^{WT} and UCH-L1^{I93M} were significantly inhibited by 3-MA treatment (Fig. 2, *C* and *D*). These results suggest that macroautophagy is one of the major pathways that degrade UCH-L1 in our cell model.

The Interactions of UCH-L1 with LAMP-2A, Hsc70, and Hsp90 Are Enhanced by the I93M Mutation in UCH-L1 and Are Independent of the Interaction between Monoubiquitin and

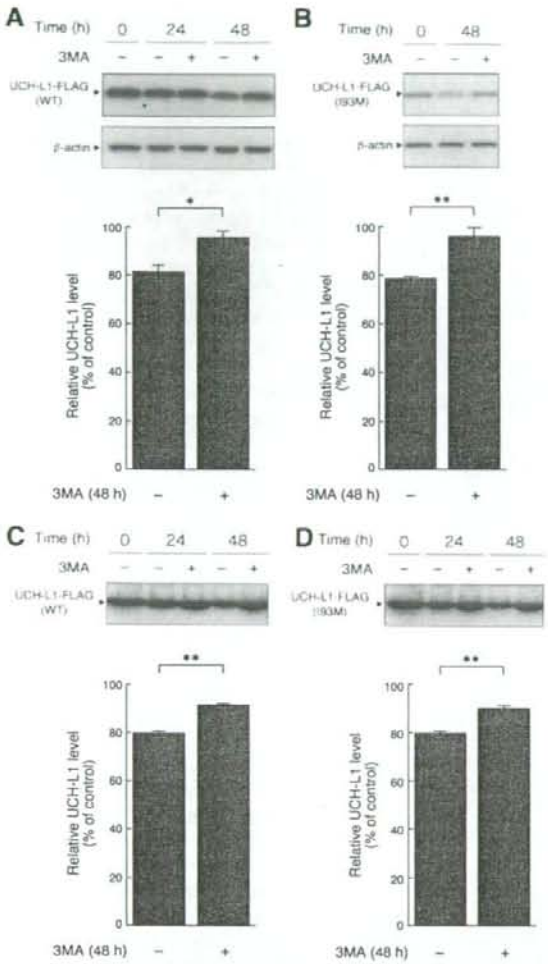

FIGURE 2. **Degradation of UCH-L1 by macroautophagy.** *A* and *B*, COS-7 cells were transfected with pTet-Off and pTRE-Tight-hUCH-L1^{WT} (*A*) or pTRE-Tight-hUCH-L1^{I93M} (*B*). Twenty-four h after transfection, transcription of UCH-L1-FLAG gene was suppressed by adding 100 ng/ml doxycycline and incubating for 4 h. Then, 3-MA (+) or vehicle (−) was added, and cells were harvested at the indicated times after the suppression of the gene and analyzed by immunoblotting (*upper panels*). The relative levels of UCH-L1-FLAG at 48 h after the suppression (% of 0-h control) were quantified by densitometry. Mean values are shown with S.E. (*A*, $n = 4$; *B*, $n = 3$). *, $p < 0.05$; **, $p < 0.01$. *C* and *D*, COS-7 cells were transfected with pCI-neo-hUCH-L1^{WT}-FLAG (*C*) or pCI-neo-hUCH-L1^{I93M}-FLAG (*D*). Twenty-four h after transfection, cells were labeled with [^{35}S]Met and [^{35}S]Cys. Autoradiograms of anti-FLAG immunoprecipitates pulse-chased at the indicated times in the absence or presence of 3-MA are shown (*upper panels*). Relative band intensities at 48 h (% of 0-h control) are quantified. Mean values are shown with S.E. ($n = 3$). **, $p < 0.01$.

UCH-L1—We have previously shown that the amount of each protein interacting with UCH-L1^{I93M} is mostly higher than the amount interacting with UCH-L1^{WT} (13). Consistent with this observation, we found that the amount of LAMP-2A, Hsc70, and Hsp90 interacting with UCH-L1^{I93M} is higher than the amount interacting with UCH-L1^{WT} (~1.8-, 1.3-, and 1.3-fold increases, respectively) (Fig. 1, *C* and *D*, and supplemental Fig. S2*A*). The interactions of LAMP-2, Hsc70, or Hsp90 with UCH-L1^{S18Y}, UCH-L1^{D30K}, which lacks hydrolase activity and binding affinity for ubiquitin (21), and UCH-L1^{C90S}, which lacks hydrolase activity but maintains binding affinity for ubiquitin (21), were not notably changed compared with those of UCH-L1^{WT} (Fig. 1*C*, supplemental Fig. S2*A*, and data not shown). These results suggest that the interaction between UCH-L1 and CMA machinery is independent of both UCH-L1-binding affinity for ubiquitin and the hydrolase activity of UCH-L1. To further show that these interactions are independent of monoubiquitin binding to UCH-L1, and to elucidate the amino acid residues of UCH-L1 involved in the interaction with LAMP-2A, Hsc70, and Hsp90, we performed coimmunoprecipitation assays using a series of alanine substitutions (13) of basic and acidic residues located on the surface of UCH-L1 (Fig. 3*A*). The R63A mutant displayed increased levels of interactions with LAMP-2, Hsc70, and Hsp90, whereas other mutations had no notable effect on the interactions (Fig. 3*A*). We further performed alanine-scanning mutagenesis experiments and found that E174A, D176A, and H185A mutants also displayed increased levels of interactions with LAMP-2, Hsc70, and Hsp90 (Fig. 3*B* and data not shown). Glu^{174}, Asp^{176}, and His^{185} are located near Arg^{63} (Fig. 3*C*). The surface region containing Arg^{63} and His^{185} possesses features that are characteristic of a protein-protein interacting site (35). These observations suggest that this surface region, which is distinct from the ubiquitin-binding region (13, 35), is involved in the interactions with LAMP-2, Hsc70, and Hsp90. The R63A, E174A, D176A, or H185A mutation possibly causes partial misfolding, resulting in increased interactions.

UCH-L1 Directly Interacts with the Cytoplasmic Region of LAMP-2A—LAMP-2 is a type 1 membrane protein, consisting of a short cytoplasmic tail (12 amino acids), one transmembrane domain, and a glycosylated luminal domain (31). To test whether UCH-L1 directly interacts with the cytosolic region of LAMP-2A, we prepared purified recombinant wild-type and I93M UCH-L1 proteins, a peptide containing an amino acid sequence corresponding to the C-terminal cytoplasmic tail of LAMP-2A, and a control peptide (Fig. 4*A*). Purified UCH-L1 proteins and the peptides were mixed, and pulldown assays were performed. A direct interaction between wild-type UCH-L1 and the cytosolic region of LAMP-2A was observed (Fig. 4, *B* and *C*). Consistent with the results of the coimmunoprecipitation assay, UCH-L1^{I93M} exhibited an abnormally increased level of interaction with the cytosolic region of LAMP-2A compared with wild-type UCH-L1 (Fig. 4*D*). Because chaperones, including Hsc70, are considered to be required for the interaction of the CMA substrates with LAMP-2A (36), our results may indicate that UCH-L1 interacts with LAMP-2A in a manner different from the interaction between CMA substrates and LAMP-2A.

UCH-L1^{I93M} Causes Accumulation of α-Synuclein—It has been reported that α-synuclein^{WT} is a CMA substrate, but pathogenic mutants A30P and A53T α-synuclein inhibit CMA by tight binding to LAMP-2A (24). Thus, UCH-L1^{I93M}, which exhibits elevated interactions with LAMP-2A, Hsc70, and Hsp90, may also inhibit CMA. To examine this possibility in mammalian cells, we assessed the effects of UCH-L1^{I93M} on the

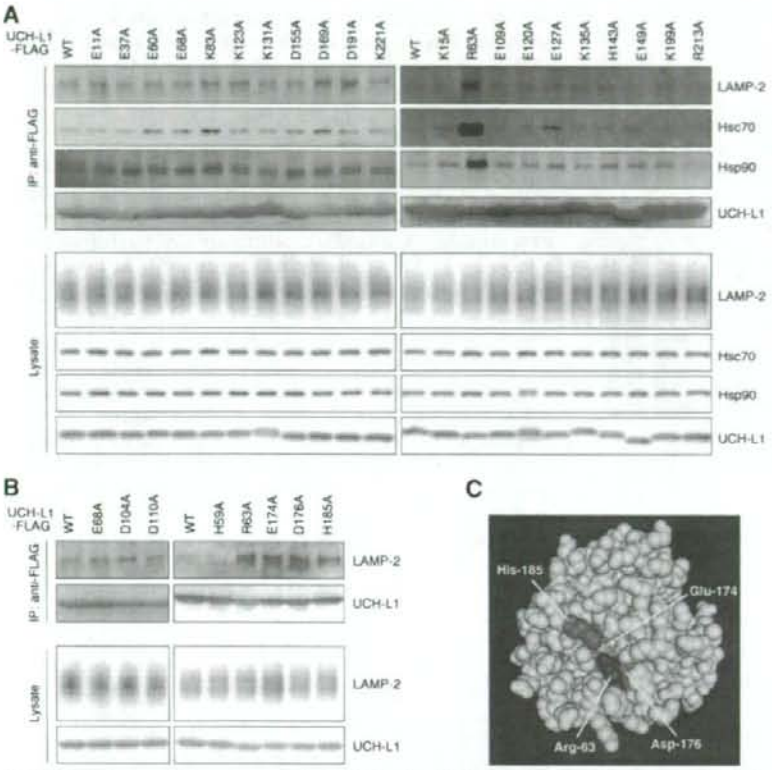

FIGURE 3. **Alanine-scanning mutagenesis of UCH-L1.** *A* and *B*, lysates of COS-7 cells transfected with the indicated constructs were immunoprecipitated (*IP*) with anti-FLAG antibody and analyzed by immunoblotting. *C*, a structural model for human UCH-L1 is shown. Arg^{63}, Glu^{174}, Asp^{176}, and His^{185} are shown in *blue*, *green*, *magenta*, and *red*, respectively, using Cn3D software (version 4.1) and NCBI structural model mmdbId:38174 (35).

protein level of GAPDH, an established substrate of CMA (24), in the lysosomal fraction and whole-cell lysate. The GAPDH level in whole-cell lysate was increased in cells expressing UCH-$L1^{I93M}$ compared with that in cells expressing UCH-$L1^{WT}$ (an ~1.5-fold increase) (Fig. 5*A*), whereas the GAPDH level in the lysosomal fraction was decreased in cells expressing UCH-$L1^{I93M}$ (an ~2.1-fold decrease) (Fig. 5*B*), supporting the idea that the aberrant interaction of UCH-$L1^{I93M}$ with CMA machinery inhibits CMA. The inhibition of CMA also results in the accumulation of other CMA substrates, including α-synuclein (24). We found that the amount of α-$synuclein^{WT}$ was increased in cells expressing UCH-$L1^{I93M}$ compared with cells expressing UCH-$L1^{WT}$ (~1.7 and 1.4-fold increases, respectively) (Fig. 5, *C* and *D*) or control mock cells (data not shown). The physical interaction between UCH-L1 and α-synuclein was not detected under these experimental conditions (data not shown). These results suggest that the accumulation of α-synuclein in cells expressing UCH-$L1^{I93M}$ is due to the inhibition of CMA-dependent degradation of α-synuclein. α-Synuclein contains a CMA recognition motif, ^{95}VKKDQ^{99}, and mutant α-$synuclein^{\Delta DQ}$, in which ^{98}DQ^{99} is replaced by Ala-Ala, is not degraded by CMA (24). To confirm that the accumulation of α-synuclein in cells expressing UCH-$L1^{I93M}$ is associated with CMA-dependent degradation of α-synuclein, we used mutant α-$synuclein^{\Delta DQ}$ and found that the I93M mutation does not affect the α-$synuclein^{\Delta DQ}$ level (~1.0 and 1.0-fold increases, respectively) (Fig. 5, *E* and *F*).

G93A Cu,Zn-superoxide dismutase 1 and WT Cu,Zn-superoxide dismutase 1 are not presumable substrates for CMA because Cu,Zn-superoxide dismutase 1 does not contain a KFERQ-like motif, but they can be degraded by the proteasome and macroautophagy (28). Protein levels of G93A Cu,Zn-superoxide dismutase 1 and WT Cu,Zn-superoxide dismutase 1 in cells transfected with UCH-$L1^{I93M}$ were not increased compared with those in cells expressing UCH-$L1^{WT}$ (an ~1.0-fold increase) (Fig. 5*G* and data not shown), suggesting that the I93M mutation does not considerably affect the degradation of proteins by macroautophagy and the proteasome under these experimental conditions.

Contrary to UCH-$L1^{I93M}$, UCH-$L1^{D30K}$ and UCH-$L1^{C90S}$ did not increase the amount of α-synuclein in cells (supplemental Fig. S2*B*), indicating that the accumulation of α-synuclein in cells expressing UCH-$L1^{I93M}$ is independent of the hydrolase activity of UCH-L1 and the interaction between monoubiquitin and UCH-L1. These observations are consistent with the results showing that the interaction between UCH-L1 and LAMP-2A, Hsc70, or Hsp90 is independent of the enzymatic activity of UCH-L1 and the interaction between monoubiquitin and UCH-L1 (Figs. 1*C* and 3) and also with the idea that the main cause of UCH-$L1^{I93M}$-associated PD is not a loss of UCH-L1 function but an acquired toxicity of UCH-$L1^{I93M}$.

DISCUSSION

An increase in the amount of α-synuclein protein could constitute a pathogenic factor underlying sporadic PD because the heterozygous duplication of the α-synuclein gene causes familial PD (4, 5), and the deposition of α-synuclein protein is associated with sporadic PD (7, 8, 37). α-$Synuclein^{WT}$ is a CMA substrate, but mutant A30P and A53T α-synuclein inhibit CMA by aberrant tight binding to LAMP-2A (24). Thus, inhibition of CMA by mutant α-synuclein might result in an increase in the amount of α-synuclein protein, leading to the neurodegeneration in familial PD associated with mutant α-synuclein. To date, the relationships between α-synuclein and other familial PD-